ELECTROCHEMICAL STUDIES ON RUTILE CATALYSTS

MIKIO MIYAKE

JANUARY, 1977

Department of Applied Chemistry
Faculty of Engineering
Osaka University

PREFACE

The works in this thesis were carried out under the guidance of Professor Hideo Tamura at Faculty of Engineering, Osaka University.

This thesis describes some electrochemical investigations on photocatalytic reactions on semiconducting rutile. The author wishes that the electrochemical methods presented in this work become one of a powerful tools on analyzing some photocatalytic reactions on semiconductor catalysts.

Mikio Miyake

Department of Applied Chemistry
Faculty of Engineering
Osaka University
Suita, Osaka

January, 1977

CONTENTS

CHAPTER 1

GENERAL INTRODUCTION

The electrochemistry of semiconductors has been emerged from a paper by Brattain and Garrett in 1955.[1] Since then, a large number of research works have been published on semiconductor electrodes,[2-5] and a new field in the electrochemistry has been developed. One of the most interesting features of the semiconductor electrochemistry is phenomena associated with illuminated electrodes.[2-5] For example, a " photo-sensitized electrolytic reaction" [6] has been found, which led to an invention of a photo-electrochemical cell.[7]

In this thesis, thories and techniques established on the semiconductor electrochemistry are applied to investigate photocatalytic reactions on a semiconductor catalyst (chapters 2-4). It is well known that catalysts play an important role in chemical reactions. It is suggested by many studies on semiconductor electrode reactions that the electrochemical method has a great advantage in elucidating whether catalytic reactions proceed via exchange of electronic carriers between catalysts and reactants or not.[4,5] A few studies have already shown that this method will be useful to analyze mechanism of catalytic reactions, if it is controlled by the exchange of electronic carriers.[8]

A photo-electrochemical cell on the conversion of solar energy into electrical energy is a very attractive device, if one thinks of energy

strage in the near future.[9] In chapters 5 and 6 of this thesis, a correlation between photo-electrochemical cell reactions and photocatalytic reactions on a semiconductor catalyst is investigated.

In this thesis, n-type semiconducting rutile was adopted as the catalyst as well as the electrode, since this material is electrochemically stable[6] and its catalysis is a problem under investigation in the research field of catalysis.[10,11]

The contents of this thesis are composed of the following papers.

1) Two Step Oxidation Reactions of Alcohols on an Illuminated Rutile Electrode

   M. Miyake, H. Yoneyama and H. Tamura,

   Chem. Lett., 635 (1976).

2) The Development of Photo-electrochemical Cells from Systems with Photocatalytic Reactions

   M. Miyake, H. Yoneyama and H. Tamura,

   Electrochim. Acta, 21, 1065 (1976).

3) An Electrochemical Study on Reactions of Quinones in Methanol on an Illuminated Rutile Catalyst

   M. Miyake, H. Yoneyama and H. Tamura,

   Electrochim. Acta, in press.

4) Correlation between Photo-electrochemical Cell Reactions and Photocatalytic Reactions on Illuminated Rutile

   M. Miyake, H. Yoneyama and H. Tamura,

   Bull. Chem. Soc. Japan, in contribution.

5) An Electrochemical Study on Photocatalytic Oxidation of Methanol on Rutile

   M. Miyake, H. Yoneyama and H. Tamura,

   J. Catal., in contribution.

6) Effect of Solution pH on the Oxidation of Alcohols on an Illuminated Rutile Anode

M. Miyake, H. Yoneyama and H. Tamura,

Denki Kagaku, in contribution.

CHAPTER 2

OXIDATION REACTIONS OF ALCOHOLS ON ILLUMINATED RUTILE

2-1 INTRODUCTION

Morrison et al. found that the anodic photo-current on an n-type ZnO electrode increased up to twice when some multi-equivalent reducing agents (e.g. alcohol, formate and As^{3+}) were added in the electrolyte solution.[12] They termed this phenomenon as the " current doubling" effect. This effect has been interpreted as the result in the two step oxidation of the reducing agent as shown in Fig. 2-1, i.e. the reducing agent R: is oxidized by the positive hole in the valence band of the semiconductor (Eq. 2-1), and the produced intermediate radical $R\cdot^{+}$, which has high electronic energy, is subsequently oxidized to R^{2+} by injecting electron into the conduction band (Eq. 2-2). Similar " current doubling" effects were reported on some semiconductor electrodes not only for the oxidation process,[13-15] but also for the reduction one.[16,17] However no report has been published on rutile.

Therefore, to clarify the mechanism of oxidation reactions of alcohols on illuminated rutile, the " current doubling" effect is investigated. Furthermore, factors which control the reactivity of the alcohols are pursued.

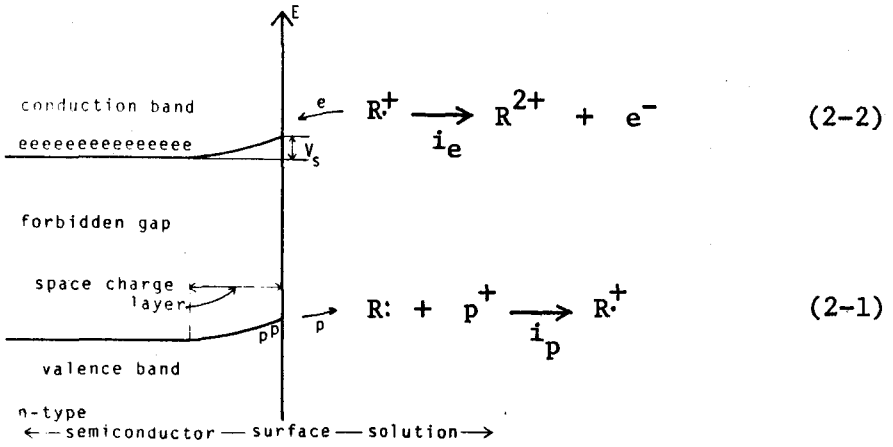

Fig. 2-1. Schematic diagram of the "current doubling" process.

2-2 EXPERIMENTAL

A rutile single crystal (10 x 10 x 3 mm) was obtained from Nakazumi Crystal Co. Ltd.. It was an as-grown one prepared by the Vernuile method and had a grey color. The (110) face was chosen as the electrode surface. Indium was electroplated on the back face of the crystal to get an ohmic contact.[6] The crystal was covered with epoxy resin except for the electrode surface and fixed in a glass tube. Before measurements, the electrode was dipped in concentrated nitric acid for 1 min, and then washed with de-ionized water for about 30 min.

Solutions used were water, methanol, ethanol, 2-propanol, 1-propanol and t-butyl alcohol containing 0.1 M HCl as the supporting electrolyte except for the experiments with different pH solutions. Water was distilled twice. Aqueous buffer solutions containing 50 volume % of alcohol were prepared by dissolving either one or two of HCl, KH_2PO_4, KCl and NaOH, and pH values of them were checked with a pH meter (Hitachi-Horiba,

M-5). There is no assurance that the hydrogen ion concentration in an aqueous solution is equal to that in the alcoholic solution used in the present study even when the indication value of the pH meter is the same between the two kind of the solutions. However, this brings no serious problem in the present study, since only qualitative information on the hydrogen ion concentration was required. Nitrogen gas bubbled into the solution was purified by passing commercial 99.99 % nitrogen over a hot copper powder and molecular sieves in the same manner as reported.[18] All chemicals used were of guaranteed reagent grade.

Anodic photo-current was measured at 2.0 V vs. S.C.E. by means of a potentiostat (Hokutodenko Ltd., model ps-500B). The differential capacitance was measured by using an a.c. bridge at 1 kHz in the dark.[19]

The rutile electrode was illuminated by a 500 W ultra-high pressure marcury arc lamp (Ushio Electric Inc., model UI-501). The light of wave length shorter than 350 nm was cut off by setting a convex glass lens in front of a qualtz window of an electrolytic cell. The intensity of the light was changed by using a glass lens or Ni nets.

A qualtz cell (volume 80 cm^3) used in the measurements had a shape of a beaker. It had a flat qualtz window, a gas inlet and an outlet in the side wall. The cell was covered with a black vinyl tape except for the window. It was connected by a solution bridge to an another beaker type cell containing the same solution, and the latter cell was connected to a reference electrode S.C.E. through an agar salt bridge. The rutile test electrode, a pt counter electrode (3 x 4 cm) and the solution bridge having a Luggin capillary were fixed in a Teflon stopper, and set in the electrolytic cell.

Formaldehyde, which was produced during the electrode reaction, was detected by colorimetry using phenyl-hydrazine.[20]

2-3 RESULTS AND DISCUSSION

Anodic process on an illuminated rutile electrode in aqueous solution without alcohol is decomposition of water by positive holes.[6)]

$$2\,H_2O + 4\,p^+ \xrightarrow[i_{po}]{} O_2 + 4\,H^+ \qquad (2\text{-}3)$$

In this case, the saturated anodic current i_{po} is controlled by the annihilation of positive holes to the reactant. On the other hand, anodic process of the " current doubling" agent is expressed by Eqs. 2-1 and 2-2 in Fig. 2-1, and the saturated anodic current, which was observed in the potential region between 1 and 3 V vs. S.C.E., is the sum of the saturated hole current i_p and the electron injection current i_e into the electrode. Accordingly, the anodic current of the " current doubling" agent increases by the factor of $(i_p + i_e)/i_{po}$ compared with i_{po}. Thus, reactivity of the " current doubling" agent can be determined by measuring $(i_p + i_e)/i_{po}$.

Figure 2-2 shows the plots of $(i_p + i_e)/i_{po}$ versus alcohol molar fraction in water for four kinds of alcohols. In this experiment, rather high photo-intensity was adopted, since the visible decomposition of rutile could not be observed. The saturated anodic current was about 500 μA in 0.1 M HCl-water. In the case of 0.1 M HCl alcoholic solution, the anodic current was greatly increased depending on the alcohol concentration except for t-butyl alcohol. This result shows that the " current doubling" takes place on the rutile electrode for the oxidation of methanol, ethanol and 2-propanol. t-Butyl alcohol, which has no α hydrogen, cannot be oxidized through the " current doubling" process as reported on ZnO.[21)] The anodic current became saturated in the solution having alcohol more than about 0.7 in molar fraction, and the magnitude of the saturated current,

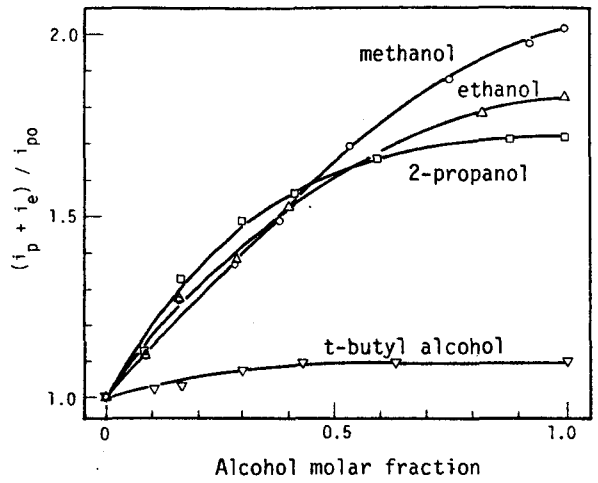

Fig. 2-2. Plots of $(i_p + i_e)/i_{po}$ vs. alcohol molar fraction.

i.e. the reactivity, decreased in the order, methanol > ethanol > 2-propanol. In the concentration region in which a strong dependency of $(i_p + i_e)/i_{po}$ was observed, no distinction of difference in the reactivity was possible among the three kinds of alcohols within experimental errors.

The number of α hydrogen of alcohols seemed to have little influence on the reactivity of the alcohols, because the reactivity of 1-propanol did not coincide with that of ethanol, but coincided with that of 2-propanol.

Judging from dissociation energies of the homopolar α hydrogen bond of the alcohols, the energy of the first step for the oxidation of the alcohols represented by Eq. 2-1 seems not to be different so much.[22] On the other hand, the result of the Mott-Schottky plots of differential capacitance showed that the flat-band potential V_{fb} of the rutile electrode in each alcohol solution without water was the same value of 0.18 V vs. S.C.E.. In this case, V_{fb} seems to be controlled mainly by the H^+ concentration in the solution.[23] Accordingly, the energy level of the valence band edge E_v at the surface of rutile in each alcohol solution would be approximately the same. These results indicate that the reactivity of the alcohols would

not be controlled by the relative energy position between the alcohols and E_v.[3,24]

To find out the reason of the difference in the reactivity by the kinds of alcohols, $(i_p + i_e)/i_{po}$ versus methanol molar fraction was plotted with various photo-intensities in Fig. 2-3. A linear relation was reported between the photo-intensity and the saturated hole current on a rutile electrode.[6] Then, a relative photo-intensity was determined by measuring the saturated hole current in 0.1 M HCl-water. In Fig. 2-3, the photo-intensity indicated as 100 in a.u. corresponded to 500 μA on the rutile electrode. The results in Fig. 2-3 as well as in Fig. 2-2 showed that $(i_p + i_e)/i_{po}$ was controlled by the amount of the alcohol in water when the alcohol concentration was rather low, and that $(i_p + i_e)/i_{po}$ was saturated when the alcohol concentration was high. The agitation of the solution did not cause the increase in the current, so the mass transfer of alcohol from the bulk solution to the surface was not important in this system.

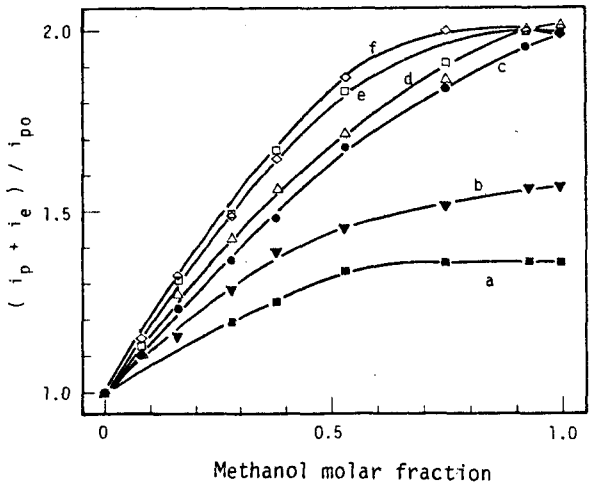

Fig. 2-3. Plots of $(i_p + i_e)/i_{po}$ vs. methanol molar fraction with various photo-intensities. Photo-intensities are (a): 340, (b): 180, (c): 100, (d): 33, (e): 14 and (f): 5 in a.u.

Therefore, we think that the reaction would be controlled by the amount of adsorbed alcohol on the rutile electrode when the alcohol concentration is less than 0.5 in molar fraction. On the other hand, the behavior in the saturation region in Fig. 2-3 should be discussed by taking into consideration of photo-intensity. When the photo-intensity was rather weak such as in the cases of the curves (d) to (f), $(i_p + i_e)/i_{po}$ began to saturate at lower methanol concentrations, since the less holes were available for the oxidation of methanol. The anodic current is not controlled by the amount of adsorbed alcohol, but controlled by the number of holes at the surface of rutile. However, when the photo-intensity was high such as in the cases of the curves (a) to (c), the anodic current seems to be affected by the amount of adsorbed methanol, since $(i_p + i_e)/i_{po}$ decreased in spite of high availability of positive holes, and i_e, which was estimated by the subtraction of i_{po} from $(i_p + i_e)$, was roughly the same for the three curves. The curves in Fig. 2-2 were measured at the same photo-intensity as the curve (c) in Fig. 2-3. Therefore, the difference in the reactivity by the kinds of alcohols would be caused by the difference in the amount of adsorbed alcohols on active sites at the surface of rutile. Some reports have been published for the adsorption of alcohols on rutile[25] and metal oxides.[26] They supported the result described above, i.e. the amount of adsorbed alcohols decreased in the order, methanol > ethanol > 2-propanol.

Figure 2-4 shows the dependence of $(i_p + i_e)/i_{po}$ on solution pH for the cases of methanol and 2-propanol. It was found that $(i_p + i_e)/i_{po}$ became high with a decrease in pH values of the solutions. Gerischer and Rösler proposed a mechanism of the " current doubling" at CdS anodes, which fitted in their experimental results that the " current doubling" was observed in a quite limited high pH region of solutions.[15]

$$R_1R_2\ C(OH)(H)_{ad} + OH^- + p^+ \longrightarrow R_1R_2\ \dot{C}(OH)_{ad} + H_2O \qquad (2\text{-}4)$$

$$R_1R_2\ \dot{C}(OH)_{ad} + OH^- \longrightarrow R_1R_2\ C{=}O + H_2O + e^- \qquad (2\text{-}5)$$

where R_1 and R_2 are H or alkyl groups. The results shown in Fig. 2-4 indicate, however, that this mechanism does not fit in the rutile electrode.

Importance of the degree of dissociation of " current doubling" agents in solutions was reported for the case of the " current doubling" reduction of H_2O_2 and p-benzoquinone on illuminated p-GaP.[16,17] Judging from a rather high pK value of methanol of 16.7,[27] almost all methanol seems to be in a molecular form and no noticeable effect of the dissociation is expected in the pH region studied. The same situation seems to be true for 2-propanol.[27] Therefore, the pH dependence of the reactivity of alcohols should be brought about by an another factor.

It is believed that the rutile surface is usually covered with OH as well as water molecules[28,29] and that the following dissociation equilibrium is established in an aqueous solution.[23,30]

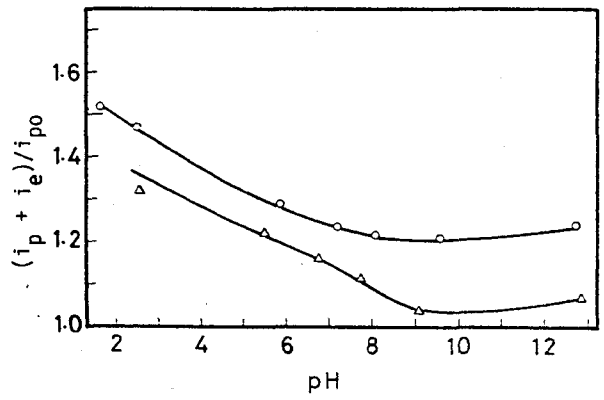

Fig. 2-4. Plots of $(i_p + i_e)/i_{po}$ vs. pH of buffer aqueous solutions with 50 volume % of alcohol. (○): methanol (△): 2-propanol

$$-Ti\text{-}OH \rightleftharpoons -Ti\text{-}O^- + H^+ \qquad (2\text{-}6)$$

$$-Ti\text{-}OH \rightleftharpoons -Ti^+ + OH^- \qquad (2\text{-}7)$$

The point of zero charge of rutile, at which the numbers of $-Ti^+$ sites are equal to those of $-Ti\text{-}O^-$ sites, was reported to lie at pH 6.0 at room temperature,[31] and $-Ti^+$ sites become abundant with a decrease of pH value of the solution.[23,30] In our experimental condition with high anodic polarization, $-Ti^+$ sites will be occupied with OH^- or H_2O to evolve oxygen if there is no specific adsorbate such as alcohols in aqueous solutions. -Ti-OH sites may also be oxidized to something like -Ti=O, as is usually believed at metal electrodes in aqueous solutions.[32] When alcohols are added into the solutions, they can adsorb on the sites of rutile surface. An alcohol molecule is considered to adsorb on a pair of bare $-Ti^+$ and $-Ti\text{-}O^-$ site, and a strong adsorption is suggested on $-Ti^+$ site of the rutile surface compared with that on $-Ti\text{-}O^-$ site.[28,33] Therefore, it is concluded that the high reactivity of alcohols in a low pH region is considered to be resposible for an increase in the number of active sites ($-Ti^+$) at the rutile surface.

The flat-band potential of rutile was reported to shift to a cathodic direction by 59 mV with an increase of unit pH.[23] When the rutile electrode is polarized at the fixed potential (2 V vs. S.C.E.) in the solutions with different pH values, magnitude of the band bending must be different depending on solution pH, and high for high solution pH. If the adsorption is affected by the electric field of the space charge formed in the electrode, a high amount of adsorption of alcohol should be observed in alkaline solutions. The result in Fig. 2-4, however, shows an inverse tendency for this prediction. Then, an another conclusion is drawn that

the difference in the band bending plays a minor role in alcohol adsorption on rutile in a potential region where the saturated photo-current appears.

In the present study, 0.1 M HCl was used as the supporting electrolyte. Gerischer et al. reported that such a high concentration of chloride ion was enough to suppress preferential oxidation of $HCOO^-$ on ZnO.[34] However, when 0.1 M $HClO_4$ was used as the supporting electrolyte in place of 0.1 M HCl, the same reactivity of methanol was obtained at rutile. A low adsorbability of chloride ion on the rutile surface has already been reported by Bérubé et al. who considered that this phenomenon was due to a small tendency of surface titanium ions to form complexes with chloride and oxyanions.[35] Their result is qualitatively in good agreement with our present result that chloride ions in the electrolyte did not supress the oxidation of the alcohols.

Rutile and ZnO are quite resemble with each other in their band gap energies and flat-band potentials.[36] However, one can find an another example of difference in electrochemical properties between rutile and ZnO. In the case of the " current doubling" oxidation of methanol on illuminated ZnO, such a small concentration of methanol as 2×10^{-2} M was enough to give preferential oxidation of alcohols, i.e. $(i_p + i_e)/i_{po} = 2$, in 1 M KCl + 0.05 M KOH aqueous solutions.[21] On the other hand, as was shown in Fig. 2-2, the concentration of more than 15 M of alcohols were necessary to be preferentially oxidized on rutile. This difference may be connected to the difference in surface conditions between ZnO and rutile. The fact that ZnO is anodically dissolved, while rutile is not, would bring about a completely different surface condition in the anodically polarized electrodes.

According to Eqs. 2-1 and 2-2, the oxidation product of alcohols through the " current doubling" process would be corresponding aldehydes

or ketones.[15,21] To examine the product, 0.1 M HCl-methanol solution without water was electrolyzed at 2.0 V using H-type cell with the same photo-intensity as in Fig. 2-2. Formaldehyde was found to be produced with 70 % of the Faradaic efficiency. Therefore, the mechanism of this reaction is described as,[13]

$$CH_3OH + p^+ \longrightarrow \dot{C}H_2OH + H^+ \qquad (2\text{-}8)$$

$$\dot{C}H_2OH \longrightarrow HCHO + H^+ + \dot{e}^- \qquad (2\text{-}9)$$

Formaldehyde and formate were reported to be oxidized by the "current doubling" process on a ZnO electrode.[21] However, similar plots as in Fig. 2-2 for formaldehyde and formate on the rutile electrode led to the result that their reactivity were lower than that of methanol, and the values of $(i_p + i_e)/i_{po}$ were less than 1.5. This result supported the fact that the major product of the oxidation of methanol on rutile was formaldehyde, and a part of formaldehyde produced seems to be oxidized further.

CHAPTER 3

AN ELECTROCHEMICAL STUDY ON REACTIONS OF QUINONES IN METHANOL ON AN ILLUMINATED RUTILE CATALYST

3-1 INTRODUCTION

Vol'kenstein developed an electron theory of catalysis on semiconductors[37] and compared his theory with experimental results.[38] Many other studies also suggest that electronic factors play an important role in catalytic reactions.[39-41] Morrison et al. investigated a photocatalytic reaction of formate in an aqueous solution on ZnO by applying electrochemical measurements.[12] Later, applicability of electrochemical techniques for investigating catalytic reactions on semiconductors was reviewed by Freund et al..[8] Recently, electrochemical measurements based on the local cell process were applied to investigate a photocatalytic reaction on rutile, and it was found that the method was useful to estimate rate and mechanism of photocatalytic reduction of methylene blue dissolved in methanol.[42]

According to the theory by Gerischer of semiconductor electrode reactions, relative position of the energy levels of the band edges of semiconductors to that of redox species in the electrolyte solution determines feasibility of electron exchange between the semiconductor and the species in the electrolyte.[43-45] Therefore, if the energy levels of the band edges are fixed, rates of electron exchange should be varied

depending on the redox-potentials of the reactants. This theory has been confirmed by the experimental results.[24,36,46-48)]

In this chapter, rates of photocatalytic reactions of quinones in methanol on an illuminated rutile catalyst and mechanisms of the reaction were investigated mainly by electrochemical measurements based on the local cell process. The purpose of this study was to investigate how much the reaction rates are influenced by redox-potentials of various quinones.

Catalytic reactions on semiconductors have been independently studied so far by employing various kind of techniques, especially by spectroscopic techniques, for variety of systems.[49)] The author expects that in addition to the techniques already established electrochemical analysis will be useful to elucidate reactions systematically from a point of the electronic energy levels.

3-2 EXPERIMENTAL

The rutile electrode was prepared by the same manner as described in chapter 2. Rutile powder as the catalyst, which was used in chemical experiments, was prepared from the commercial TiO_2 powder of anatase by heating at 1200°C in an argon atmosphere for over 4 hr to change into a gray colored rutile. As the powder particles stuck to each other during heating, they were crushed in an agate mortar to obtain particles which could pass through a 48 mesh screen. A Pt electrode (1 x 1 cm) used in cyclic voltammetry experiments was prepared by dipping in aqua regia, in 30 % NaOH solution, and then in conc. HCl. Before measurement, cyclic potential scans were conducted in 0.05 M H_2SO_4 in a potential range covering hydrogen and oxygen evolution until a reproducible voltammogram was obtained.

The solution used in this study was methanol containing 10^{-3} M quinone and 10^{-1} M $LiClO_4$, and nitrogen gas was bubbled before measurements for 30 min. The quinones used were tetramethyl-p-benzoquinone, p-benzoquinone, chloranil and 2,3-dichloro-5,6-dicyano-p-benzoquinone. $LiClO_4$ was dried at 150°C for about 30 hr in vaccum. All chemicals used were of guaranteed reagent grade.

Illumination intensity was determined and adjusted to 1.2 W/cm^2 with a laser power meter (Coherent Radiation Co., model 201).

Polarization measurements were carried out by using a potentiostat, and the current was recorded by an electronic polyrecorder (Toa Denpa Co., model EPR 10 A) to make certain of a stationary condition.

For chemical analysis of the photocatalytic reaction, the same cell as in the electrochemical analysis which was described in chapter 2 was used. In this case, 50 cm^3 of the methanol containing 10^{-3} M quinone and 10^{-1} M $LiClO_4$ was poured into the cell together with the rutile powder (0.23 g), and the solution was agitated with a magnetic stirrer. During the illumination, 2 cm^3 of the cell solution was intermittently sampled out for the chemical analysis, in such a manner as to prevent extraction of rutile powder from the cell, by using a special pipette with a glass filter at the mouth. Formic acid and formaldehyde were detected by colorimetry using mercuric chloride,[50] and phenyl hydrazine,[20] respectively. Carbon dioxide was absorbed in an aqueous 0.1 M NaOH solution, and then titrated with 0.1 M HCl. Absorbancy was measured by a Hitachi 124 spectrophotometer to determine the concentration of quinone in the solution.

Other details such as the light source, purification of the gas and measurements of differential capacitance were given in chapter 2.

3-3 RESULTS AND DISCUSSION

(1) Chemical Analysis

As the experiments were conducted with light of the wave length longer than 350 nm, effects of excitation of quinone itself to the results were negligible.

When the catalytic reaction on the rutile powder was nearly completed by the illumination for more than 4 hr in methanol containong 10^{-3} M p-benzoquinone and 10^{-1} M $LiClO_4$, the light yellow solution turned colorless, and became transparent to the light of 260 nm which should be absorbed by p-benzoquinone. At this stage, 8×10^{-4} M formaldehyde was detected. Though formic acid and carbon dioxide, which are the further oxidized product of methanol, were detected, their amount were small compared with that of formaldehyde. According to these results, the following reaction can be proposed as the main reaction.

(3-1)

On the other hand, if the p-benzoquinone solution was illuminated without the rutile powder, the solution retained the original color even after the illumination was done for 20 hr.

Figure 3-1 shows concentration of p-benzoquinone and chloranil as a function of the illumination time. Linear relations were established between the logarithm of the concentration of quinones and the reaction time. Similar results were obtained in the case of 2,3-dichloro-5,6-dicyano-p-benzoquinone and tetramethyl-p-benzoquinone. Hence, the reactions seem to be the first order with respect to quinones. The rate constants calculated from the slope of the lines are shown in Fig. 3-4 against the

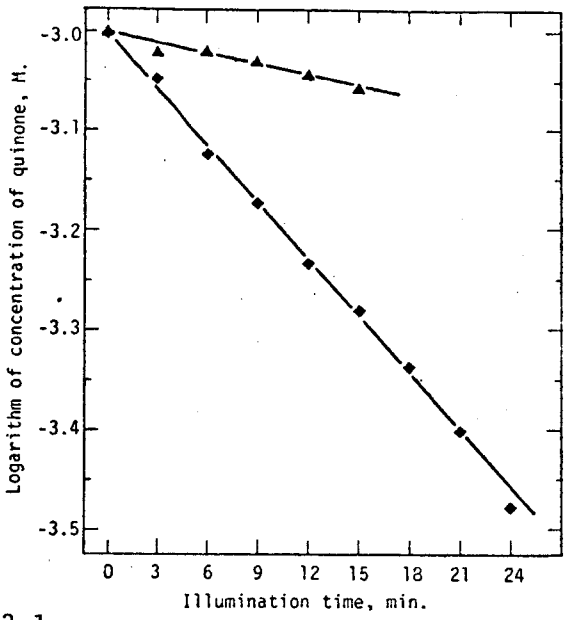

Fig. 3-1. Change of quinone concentration in 0.1 M $LiClO_4$-CH_3OH with illumination time. ▲ *p*-benzoquinone, ◆ chloranil.

reaction rates determined by the electrochemical measurements which are described in a next section. The reaction rate constants were found to be decreased in the order, 2,3-dichloro-5,6-dicyano-p-benzoquinone > chloranil > p-benzoquinone > tetramethyl-p-benzoquinone.

(2) Electrochemical Analysis

Figure 3-2 shows polarization curves of the rutile electrode in 10^{-1} M $LiClO_4$-methanol with and without 10^{-3} M tetramethyl-p-benzoquinone. In the methanol solution without quinone, both anodic and cathodic currents were small in the dark, whereas anodic current noticeably increased under illumination. In the dark, there are few positive holes in the valence band of rutile. On the other hand, when the rutile electrode is illuminated by the light having higher energy than the band gap of rutile (3.05 eV), positive holes are produced as a result of the excitation of electrons in the valence band to the conduction band. Consequently, the anodic current

observed under illumination should be connected with positive holes. The dependence of the anodic current on the light intensity supported this view.[6] It can be noticed from the comparison of the cathodic curves in Fig. 3-2 with each other that the cathodic current increased greatly by the addition of tetramethyl-p-benzoquinone in methanol solution. As for the anodic curves, however, a little change was observed between the solution with and without quinone. Therefore, the increase of the cathodic current by addition of quinone to methanol should be ascribed to reduction current of quinone, while the anodic photo-current is related to oxidation of methanol. The cathodic current increased exponentially with increase of cathodic polarization, and the cathodic curve obtained in the dark approximately coincided with the one obtained under illumination in the high cathodic potential region. These results suggest that electrons as the majority carrier in the conduction band participate in the cathodic process.[2,3]

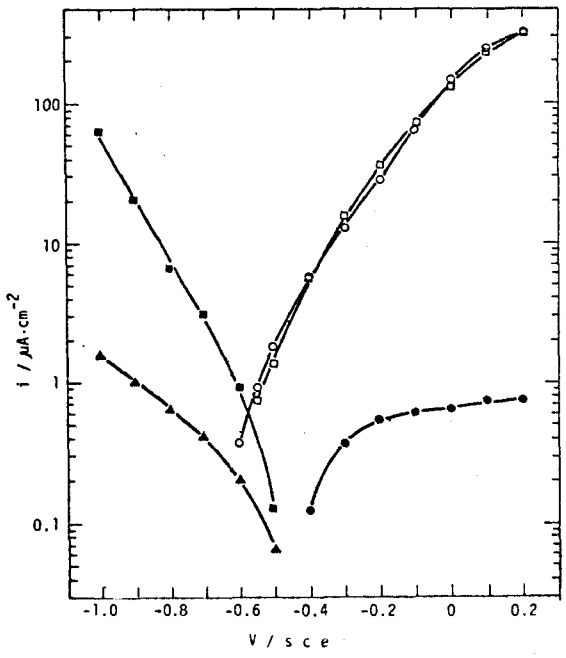

Fig. 3-2. Polarization curves of the rutile electrode in 0.1 M $LiClO_4$-CH_3OH with and without 10^{-3} M tetramethyl-*p*-benzoquinone. ○ anodic curve without quinone under illumination; □ anodic curve with quinone under illumination; ● anodic curve without quinone in the dark; ■ cathodic curve with quinone in the dark; ▲ cathodic curve without quinone in the dark.

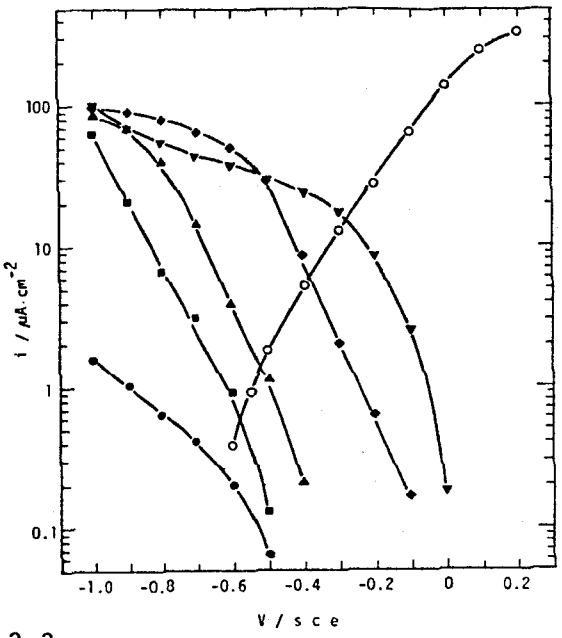

Fig. 3-3. Polarization curves of the rutile electrode in 0.1 M $LiClO_4$-CH_3OH with and without 10^{-3} M quinone. ○ anodic curve without quinone under illumination; ● cathodic curve without quinone in the dark; ■ cathodic curve with tetramethyl-*p*-benzoquinone in the dark; ▲ cathodic curve with *p*-benzoquinone in the dark; ◆ cathodic curve with chloranil in the dark; ▼ cathodic curve with 2,3-dichloro-5,6-dicyano-*p*-benzoquinone in the dark.

Similar results were obtained for polarization curves measured in other quinone solutions. The cathodic current in the dark in methanol without quinone was so small that it negligibly contributed to the cathodic curve obtained in the presence of quinone.

From the above results, the cathodic and the anodic process on illuminated rutile in methanol containing quinone are characterized by the cathodic curve obtained in the dark and the anodic curve obtained under illumination, respectively. They are summarized in Fig. 3-3 for solutions of variety of quinones.

When a photocatalytic reaction is proceeding, the catalyst must maintain electrical neutrality. This condition corresponds to the intersection point of the oxidation curve of methanol and the reduction curve of quinone in Fig. 3-3. The current value at the intersection point, thus, indicates the reaction rate, and the potential at this point shows the potential at which the reaction is proceeding (the reaction proceeding potential). The

reaction proceeding potential obtained as the intersection point coincided well with open circuit potential of the illuminated rutile electrode in the respective solution.

(3) Effects of Illumination on the Cathodic Polarization Curves

If the cathodic polarization curve obtained in the dark is not changed by the illumination, then, we can estimate the rate of the photocatalytic reaction as the current value at the intersection point of the anodic and the cathodic curves in Fig. 3-3. Then, if we can show that the electron concentration at the rutile surface is almost unchanged by the illumination, it can be said that the illumination has a negligible influence on the cathodic polarization curves. In the following, this problem is discussed.

The electron concentration at equilibrium in the rutile electrode at room temperature (n_o) was in the order of $10^{18}/cm^3$ from the knowledge of N_D value which is described in a later section. The concentration of excited electrons by the illumination (n^*) is expressed as a function of distance (x) from the illuminated surface[51] by;

$$\begin{aligned} dn^*(x)/dt &= \alpha f' \exp(-\alpha x) - di/dx - n^*(x)/\tau \\ i &= -D\, dn^*(x)/dx \end{aligned} \qquad (3\text{-}2)$$

where α, f', τ, and D denote the absorption coefficient of rutile, numbers of incident photons per cm^2 per second on the crystal, the life time of the carrier in rutile and the diffusion constant of the carrier in rutile, respectively. In a steady state, Eq. 3-2 becomes;

$$f'\alpha \exp(-\alpha x) + D\, d^2n^*(x)/dx^2 - n^*(x)/\tau = 0 \qquad (3\text{-}3)$$

since $dn^*(x)/dt = 0$.[51] By applying the conditions that $n^*(x)$ becomes 0 when x is infinitely large, and that carriers which diffuse to the surface can escape from the crystal to flow the current, that is, $i = -D(dn^*(x)/dx)_{x\to o} = n^*(x\to 0)$, Eq. 3-3 gives the following equation;

$$n^*(x) = \alpha f'\tau[\exp(-\alpha x)]/(1 - D\tau\alpha^2) + K \exp[-x/(D\tau)^{1/2}]$$
$$K = \alpha f'\tau^{3/2} (D\alpha - 1)/[(D\alpha^2\tau - 1)(D^{1/2} - \tau^{1/2})] \qquad (3\text{-}4)$$

α of rutile is judged to be 10^3~10^6/cm in the wavelength between 350 and 400 nm.[52,53] If values of 1 $cm^2/V\cdot s$ and 30 are chosen as the electron mobility [53,54] and the effective mass of an electron in rutile,[53,55] respectively, then, we can obtain 3×10^{-2} cm^2/s for D, and 9×10^{-14} s for τ, from well known equations;[56]

$$D = \mu kT/e \qquad (3\text{-}5), \qquad \tau = \mu m^*/e \qquad (3\text{-}6)$$

where μ and m^* denote the electron mobility and the mass of an electron in rutile, respectively.

The quantum yield of the "photo-sensitized electrolytic oxidation" of water is dependent on wave length and N_D, and is around 0.3 ± 0.2 at an rutile anode having 10^{18} carriers per cm^3 at 2 V vs. S.C.E. in the wave length between 350 and 400 nm.[57] If it is assumed that numbers of holes reached at the electrode surface per second are 0.1 fraction of that of incident photons, we can get a rough measure of f' from a knowledge of saturated photo-current. We use here the smallest value of the quantum yield of 0.1, because we have to estimate the upper limit of n^*. In the present study, the saturated anodic current at 2 V vs. S.C.E. in 0.1 M $LiClO_4$-methanol solution was 600 $\mu A/cm^2$. Accordingly, the saturated hole

current is estimated to be 300 $\mu A/cm^2$, if one takes into consideration of the " current doubling" effect described in chapter 2. Then, f' was judged to be less than $10^{17}/cm^2 \cdot s$.

In order to get information on concentration of photo-generated electrons at the surface, Eq. 3-4 was simplified with a condition of $x \to 0$.

$$n^*(x \to 0) = \alpha f' \tau / (1 - D\tau\alpha^2) + K \qquad (3\text{-}4')$$

By substituting the just estimated values into Eq. 3-4', $n^*(x \to 0)$ was determined to be smaller than $10^{10}/cm^3$.

Now it is possible to get information on a relative measure of numbers of photo-generated electrons at the surface of rutile to those of electrons at equilibrium in the dark. The electron concentration at the surface of the electrode (n_s) in the dark is given by Eq. 3-7.[46)]

$$[n_s] = n_o \exp [-e(V - V_{fb})/kT] \qquad (3\text{-}7)$$

where V and V_{fb} are the electrode potential and the flat-band potential of rutile, respectively. The similar argument can be applied also to $n^*(x \to 0)$ when the effect of band bending is taken into consideration for $n^*(x \to 0)$. Anyway, compared the value of n_s with that of $n^*(x \to 0)$, $n^*(x \to 0)$ is too small to give a distinct change in numbers of electrons at the rutile surface. Even if the values adopted in the above calculations are not rigidly correct, the difference between n_s and $n^*(x \to 0)$ is large enough to overcome the errors.

It may be valuable to discuss an effect of photovoltage on cathodic polarization curves obtained in the dark. A depletion layer is formed when a n-type semiconductor electrode such as rutile is contacted with a redox-electrolyte which has a more noble redox-potential than V_{fb}. By

illumination degree of the band bending is reduced, and this effect causes so-called photovoltage.[58] According to Gerischer, the electron energy level in the semiconductor is changed by illumination by the magnitude of the photovoltage, and the change is equal to $e(E_F^* - E_F)$ eV, where E_F^* and E_F denote Fermi levels of the semiconductor under illumination and in the dark, respectively.[58] If it is taken into consideration that the concentration of electrons at the electrode surface is solely determined by the band bending, then, it is possible to reproduce the band situation modified by the photovoltage, at the electrode in the dark by polarizing it by $|E_F^* - E_F|$ from E_F. This means that the degree of the band bending of the electrode is the same regardless of whether the electrode is illuminated or not, so far as the electrode is held at the same potential.

It is believed from the just described discussion that the reduction curve obtained in the dark in Fig. 3-3 represents the behavior of the reduction of the quinones on the illuminated rutile catalyst.

(4) Reaction Rates

The reaction rates determined as the current values at the intersection points in Fig. 3-3 were summarized in Fig. 3-4 against the rate constants determined by the chemical analysis. A linear correlation was obtained between the results determined by two kind of methods. One should notice, however, that the catalyst used in the electrochemical analysis was different from that used in the chemical analysis. The former was the single crystal already described, while the latter was the rutile powder having unidentified carrier concentration N_D and various crystal planes exposed to the solution. Nevertheless, the fact that the linear correlation was observed, suggests that the carrier concentration as well as the crystal plane played a minor role in determining the order of the reduction rates of various quinones.

The result shows that the reaction rates can be estimated by the electrochemical analysis.

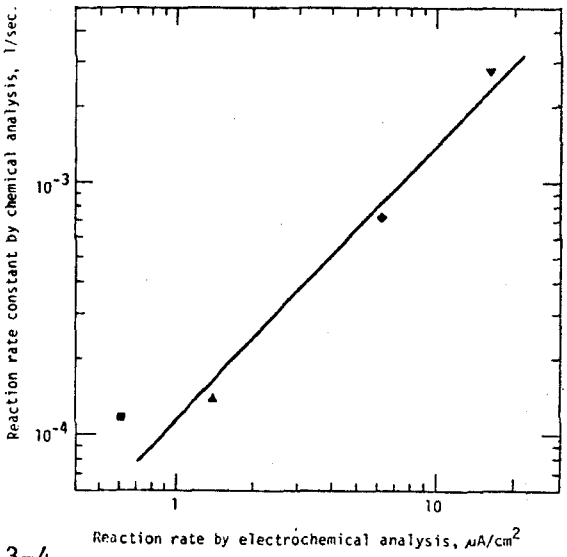

Fig. 3-4. Correlation of reaction rates of quinones dissolved in methanol determined by electrochemical analysis with reaction rate constants determined by chemical analysis. ■ tetramethyl-*p*-benzoquinone; ▲ *p*-benzoquinone; ◆ chloranil; ▼ 2,3-dichloro-5,6-dicyano-*p*-benzoquinone.

(5) Reaction Mechanism

To estimate the redox-potentials of quinones dissolved in 0.1 M $LiClO_4$-methanol, cyclic voltammograms were obtained at the Pt electrode. The obtained peak potentials for the reduction (E_{pc}) and the oxidation (E_{pa}) of quinones are given in Table 3-1. The redox reactions of quinones seem to proceed irreversibly. The tendency can be noticed that the quinone having a stronger electrophilic substituent shows a more noble redox-potential, as expected from the results on Hg in acetonitrile solutions.[59] Although

Table 3-1. Peak potentials for reductions and reoxidations of quinones in 0.1 M $LiClO_4$-methanol*

Quinone	E_{pc}	E_{pa}
Tetramethyl-*p*-benzoquinone	−0.58	−0.10
p-Benzoquinone	−0.25	−0.05
Chloranil	+0.04	+0.13
2,3-Dichloro-5,6-dicyano-*p*-benzoquinone	+0.03	+0.61

* Measured *vs sce*. Sweep rate: 200 mV/s.

redox-potentials of quinones could not be estimated exactly, it brings no serious problem in the discussion which is stated below.

Figure 3-5 shows typical Mott-Schottky plots of differential capacitance of the rutile electrode in 10^{-1} M $LiClO_4$-methanol containing 10^{-3} M p-benzoquinone in the dark. Linear relations can be observed between the plots of $1/C^2$ vs. V. Similar results were obtained in the case of 10^{-1} M $LiClO_4$-methanol without the quinone as well as with the other quinones. Although the lines in the plots of $1/C^2$ vs. V seemed to be a little influenced by the kind of quinones chosen, no definite conclusion could be drawn about this point on account of poor reproducibility. The poor reproducibility would be due to the lack of potential controlling ions, i.e. H^+, or OH^-, for a rutile electrode in the solution.[23] The behavior of the lines in Fig. 3-5, which shows strong frequence dependency, is similar to that of a rutile electrode reported by Gomes et al. in an aqueous solution, and the physical significance of the dispersion was already discussed.[60,61] The flat-band potential V_{fb} can be determined if extrapolation of $1/C^2$ vs. V to $1/C^2 = 0$ gives a constant V irrespective of the frequency chosen in the experiment. Then, we have -0.50 V as the value of V_{fb} from the result in Fig. 3-5. The

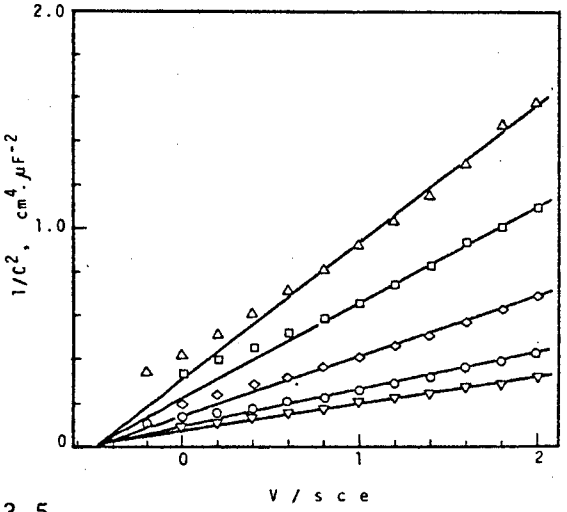

Fig. 3-5. $1/C^2$ *vs* V plots of the rutile electrode in 0.1 M $LiClO_4$-CH_3OH with 10^{-3} M *p*-benzoquinone. Measured at △ 10 kHz; □ 5 kHz; ◇ 2 kHz; ○ 1 kHz; ▽ 500 Hz.

obtained V_{fb} seems to be reasonable, since the anodic photo-current in Fig. 3-3 commences around this potential.

The energy levels of the conduction band edge at the surface of the semiconductor (E_c) was estimated from Eq. 3-8 in the same manner as reported.[24]

$$E_c = E_F - kT \ln(N_D/N_c) \qquad (3\text{-}8)$$

Carrier concentration N_D can be in principle obtained from the slope of the line of the Mott-Schottky plots. However, it was impossible to determine the correct carrier concentration in the present case on account of the frequence dependency of the slope of the plots. Judging from the result in Fig. 3-5, however, N_D of the electrode seemed to be in the order of $10^{18}/cm^3$. In the following discussion, we chose 10^{18} and $10^{19}/cm^3$ as the value of N_D. Although N_D could not be estimated precisely, it brings no serious problem in our discussion, since the same electrode was used for electrochemical measurements of various quinone solutions, and errors of one order of magnitude in N_D brings the change of the position of band edge only by 60 mV. If the density of the states at the lower band edge of the condution band (N_c) is adopted to be $2.5 \times 10^{21}/cm^3$,[53,62] then with -0.50 V of V_{fb} ($= -E_F/e$), E_c is positioned at a higher energy level by 0.67±0.03 eV than the zero electron energy level referred to S.C.E.. As the band gap of rutile is 3.05 eV,[52] the energy level of the valence band edge (E_v) is estimated to be -2.38±0.03 eV.

The energy levels of quinones are, therefore, located in the forbidden gap of rutile. The rearrangement energy λ of p-benzoquinone/hydroquinone in water was estimated by Memming et al. to be $\lambda_1 = 0.3\pm0.1$ eV, $\lambda_2 = 0.5\pm0.2$ eV.[16] These values are rather small compared with those of other

substances.[63] Anyway, if redox-potentials of quinones are located in the middle of E_{pc} and E_{pa} in Table 3-1, and if λ of quinones in methanol used in this experiments are assumed to be 0.3 eV, then, some overlapping of the bands could be found between E_c of the electrode and the quinones in the solution. To obtain strict value of λ is beyond the scope of this study. Cathodic current in Fig. 3-3 commenced at around V_{fb} or at more anodic potentials than V_{fb}, and this implys that the reduction of quinones commenced under a condition that the bands bend up toward the surface up to 0.6 eV at the largest case (2,3-dichloro-5,6-dicyano-p-benzoquinone). It was already reported that electron transfer from the conduction band to a chemical substance in solution can take place in the similar circumstance.[46,64] Therefore, reduction of quinone would be related to the conduction band electrons.

Memming et al. reported that p-benzoquinone was reduced through the " current doubling" process on Ge, Si and GaP, and that only the conduction band electrons participated in the process when SnO_2 having large band gap (3.7 eV) was used.[16] Whether the " current doubling" takes place or not in the cathodic process on a n-type rutile could not be determined. As far as experimental results obtained so far are concerned, it seems that the conduction band electron is involved at least in the first step of the reduction of quinones.

According to the theories of the semiconductor electrodes, Tafel slope of 59 mV/decade should be observed if effect of polarization is concentrated in the space charge layer of the semiconductor.[5,61] Experimental verification of this view was already done on ZnO electrodes.[46] However, each cathodic polarization curves of various quinone in Fig. 3-3 had the slope of about 170 mV/decade. This result seems to suggest that observed cathodic current was not determined purely by the electron density at the

electrode surface.

On the other hand, oxidation of methanol proceeds through the " current doubling" prodess on illuminated rutile as described in chapter 2. This process was found to be realized also on the illuminated rutile electrode in methanol containing quinones used.

Therefore, the mechanism of the photocatalytic reaction of quinones in methanol are summarized as follows.

Oxidation: $CH_3OH + p^+ \longrightarrow \dot{C}H_2OH + H^+$ (valence band) (3-9)

$\dot{C}H_2OH \longrightarrow HCHO + H^+ + e^-$ (conduction band) (3-10)

Reduction: 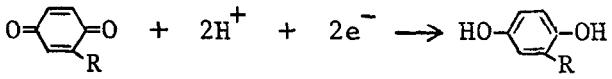 (conduction band) (3-11)

or

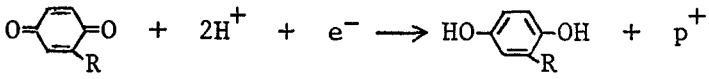 (conduction and valence bands) (3-12)

Overall: 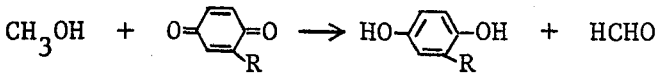 (3-13)

CHAPTER 4

AN ELECTROCHEMICAL STUDY ON PHOTOCATALYTIC OXIDATION OF ALCOHOLS ON RUTILE

4-1 INTRODUCTION

Up to the present time, photocatalytic oxidation of alcohols on ZnO and TiO_2 were studied extensively by employing variety of techniques. In 1950's, Markham et al. investigated a photocatalytic oxidation of alcohols in the presence of ZnO powder and proposed a radical chain mechanism via an intermediate complex of alcohol with oxygen.[65-67] A similar mechanism was reported by Fujita in 1961.[68] Recently, Stone and Bickley investigated a photocatalytic oxidation of gaseous 2-propanol on rutile, in which an important role of surface hydroxyl groups on oxygen adsorption was revealed.[10,69] The results obtained by them were in accord with other reports.[68,70] A reaction mechanism proposed by them was that surface OH groups trap photo-holes, and that oxygen anions formed by the reaction of photo-electrons with oxygen molecules participate in the oxidation of 2-propanol molecules.[10] More recently, the photocatalytic oxidation of 2-propanol was studied in the liquid phase by Cundall et al. using rutile suspensions.[71] They proposed a different mechanism from that by Stone et al.,[10] although the primary steps consuming photo-generated electron-holes were the same.[71]

The main products obtained in the photocatalytic oxidation of 2-propanol

on ZnO were acetone and/or propylene depending on experimental conditions.[10, 66-72] The products on TiO_2 were similar to those on ZnO except that water was detected instead of hydrogen peroxide in the case of dehydrogenation reaction of 2-propanol.[11] As for the photocatalytic oxidation of methanol on TiO_2, few reports were published. Cunningham et al. detected formation of formaldehyde and methane by using a dynamic mass spectrometer in a flash photolysis of methanol on TiO_2.[73]

In this study, a photocatalytic oxidation of alcohol by oxygen on rutile is investigated mainly by an electrochemical method based on the local cell process in the analogous manner to that described in chapter 3. The purpose of this chapter is to demonstrate applicability of the electrochemical analysis. The author expects that electrochemical methods would be one of a powerful tools to investigate catalytic reactions.

4-2 EXPERIMENTAL

The (110) face of two pieces of commercial single crystals of rutile (6 x 6 x 6 mm) of different carrier concentration N_D were used as the electrodes as well as the catalysts. Their N_D estimated from Mott-Schottky plots were judged to be in an order of 10^{19} and $10^{18}/cm^3$, respectively. Preparation of the rutile electrode (catalyst) was the same as that described in chapter 2. Two kind of surface pre-treatment procedures were adopted in the present study. Before measurement, the electrode (catalyst) was dipped in conc. nitric acid solution for 1 min, washed with de-ionized water for more than 30 min, and then dried mildly by hot air. This is one procedure. The other procedure was the same except for that rutile was finally dried thoroughly in a desiccator in vaccum at room temperature for 3 days. The rutile crystal dried in the former manner is described in this study as

" mildly dried rutile", while the latter as " thoroughly dried rutile" for the convenient purpose.

The solutions used in this study were methanol and 2-propanol containing 0.1 M $LiClO_4$ as the supporting electrolyte. Methanol and 2-propanol used were distilled twice with Mg-I_2. Purified tank nitrogen or oxygen gas was bubbled into the solution for more than 30 min before measurements.

Rutile was illuminated by a 500 W xenon arc lamp. The illumination intensity was adjusted using a standard rutile electrode so as to give an anodic photo-current of 2.1 mA at 2 V vs. S.C.E..

On chemical investigation of the photocatalytic reaction, the same measurement cell and rutile as in the electrochemical analysis were used. In this case, 60 cm^3 of 0.1 M $LiClO_4$-methanol was poured into the cell. After the rutile catalyst was set in the cell, oxygen gas was bubbled for 30 min, and then rutile was illuminated with the same photo-intensity as in the electrochemical measurements. During the illumination, 5 cm^3 of the cell solution was sampled out intermittently for chemical analysis by interrupting the illumination. After the sampling, oxygen gas was again bubbled for 10 min, and the illumination was then started. Hydrogen peroxide was detected by colorimetry using pottasium ferricyanide.[74] Absorbance was measured by a Baush & Lomb spectronic 20 spectrophotometer.

The electrochemical and chemical analysis were conducted at 25°C. Other details such as the structure of the cell, the measurement of a differential capacitance and polarization curves, purification of the gas, and detection of formic acid and formaldehyde were described in chapters 2 and 3.

4-3 RESULTS AND DISCUSSION

(1) Chemical Analysis

It was confirmed that the main oxidation product of methanol was formaldehyde. Formic acide was produced, but the amount of it was negligibly small. Figure 4-1 shows the amount of formaldehyde formed in the solution by the photocatalytic reaction on rutile as a function of the illumination time. The figure shows that the amount of formaldehyde increased linearly with the reaction time. A linear increase of the product with the reaction time is reasonable, because the reactants were in great excess compared with the resultants. The similar relation between a product and reaction time was observed by Cundall et al. in the oxidation of 2-propanol.[71] Hydrogen peroxide was produced in the liquid phase, then, the following overall reaction were feasible:

$$CH_3OH + O_2 \longrightarrow HCHO + H_2O_2 \qquad (4\text{-}1)$$

$$2\ CH_3OH + O_2 \longrightarrow 2\ HCHO + 2\ H_2O \qquad (4\text{-}2)$$

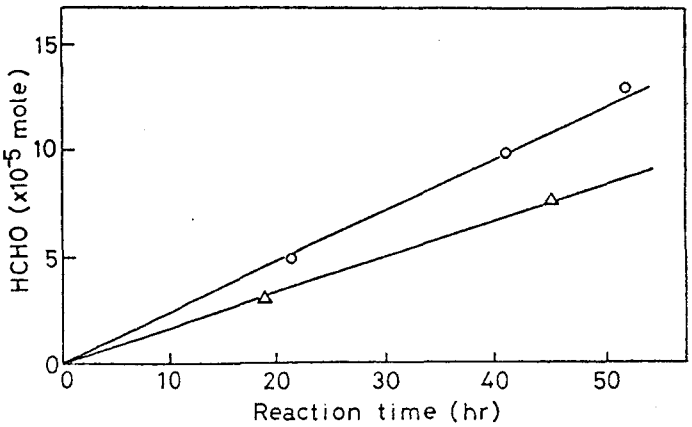

Fig. 4-1. Quantity of formaldehyde formed on mildly dried rutile catalysts as a function of illumination time in 0.1 M $LiClO_4$-CH_3OH saturated with oxygen. (○) rutile with low N_D, (△) rutile with high N_D.

The probability of the latter reaction was suggested by Stone et al.[10] and by Filimonov.[11] Our main intention was not to determine precisely the ratio of the reaction 4-1 to 4-2, but to catch information on electronic exchange between the catalyst and the reactants. By this reason, quantitative analysis of H_2O as well as H_2O_2 was not conducted.

The reaction rate was estimated from the slope of the line in Fig. 4-1 on the assumption that production of 1 mole of formaldehyde needs 2 Faradays. Thus estimated reaction rates are summarized in Table 4-1 together with the results obtained by the electrochemical analysis which is described later. When the thoroughly dried rutile was used, no definite result could be obtained because of a very low reaction rate which is suggested by the electrochemical analysis.

(2) Electrochemical Analysis

Figures 4-2 and 4-3 show polarization curves of the mildly dried and thoroughly dried rutile electrode of high N_D, respectively. In both cases,

Table 4-1. REACTION RATES DETERMINED BY THE CHEMICAL AND THE ELECTROCHEMICAL ANALYSIS

Rutile	Pre-treatment	Alcohol	Rate by chemical analysis ($\mu A/cm^2$)	Rate by electrochemical analysis ($\mu A/cm^2$)
Low N_D	Hot air	Methanol	130	140
High N_D	Hot air	Methanol	88	52
High N_D	Desiccator	Methanol	—	2
High N_D	Hot air	2-Propanol	—	5

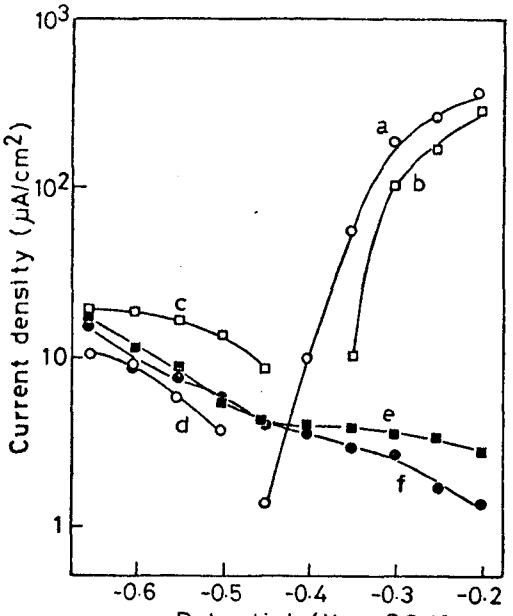

Fig. 4-2.

Polarization curves of the mildly dried rutile electrode with high N_D in 0.1 M $LiClO_4$-CH_3OH. (a) anodic curve under illumination in N_2 atmosphere, (b) anodic curve under illumination in O_2 atmosphere, (c) cathodic curve under illumination in O_2 atmosphere, (d) cathodic curve under illumination in N_2 atmosphere, (e) cathodic curve in the dark in O_2 atmosphere, (f) cathodic curve in the dark in N_2 atmosphere.

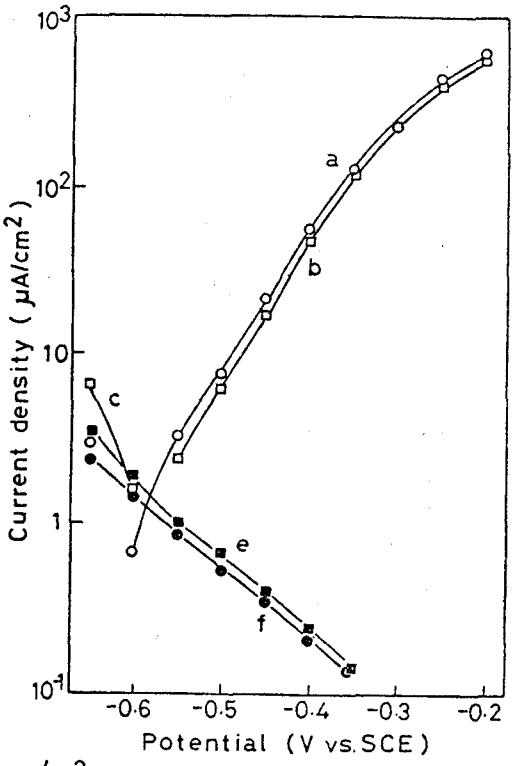

Fig. 4-3.

Polarization curves of the thoroughly dried rutile electrode with high N_D in 0.1 M $LiClO_4$-CH_3OH. Notations are the same as in Fig. 4-2

only a small anodic current was observed in the dark because of scarcity of positive holes in the valence band of rutile. Therefore, in Fig. 4-2 as well as in Fig. 4-3, the anodic polarization curve (a), obtained under illumination without oxygen in the solution, indicates the oxidation of methanol in which positive hole participates. Cathodic polarization curves obtained in the dark were not influenced by introduction of oxygen, as is observed by comparing the curve (e) with (f). This result shows that rutile in the dark is inactive for the reduction of oxygen, as was suggested from the results obtained by Stone et al..[75] However, rutile under illumination worked effectively as the catalyst. Introduction of oxygen into the solution brought about decrease of the anodic current. The decrease should be due to participation of oxygen reduction. Polarization curve of oxygen

reduction on illuminated rutile is, then, estimated by subtracting the current value of the curve (b) from that of the (a), and the curve (d) from the (c) at respective potentials. Thus obtained cathodic polarization curves of oxygen are presented in Fig. 4-4 for the case of Fig. 4-2 and in Fig. 4-5 for Fig. 4-3 together with anodic curves of methanol oxidation. Polarization curves obtained with mildly dried rutile electrode of low N_D show a similar tendency to those in Fig. 4-2.

By comparing polarization curves in Fig. 4-2 with respective curves in Fig. 4-3, it is noticed that current decrease on introduction of oxygen was very small in the case of the thoroughly dried rutile. This effect was clearly shown in the difference in the cathodic polarization curves between Figs 4-4 and 4-5. The behavior of the cathodic curves in both Figs. 4-4 and 4-5 are quite unique in the point that the cathodic current showed its maximum in the potential region where the anodic oxidation of methanol

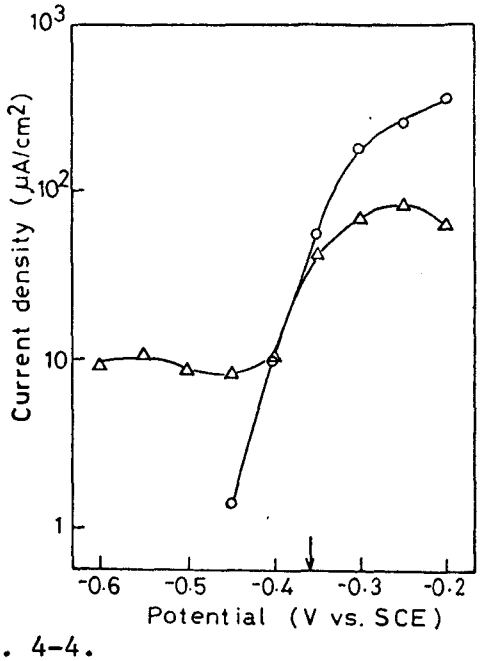

Fig. 4-4.
(o) Oxidation and (△) reduction curves of rutile obtained from Fig. 4-2

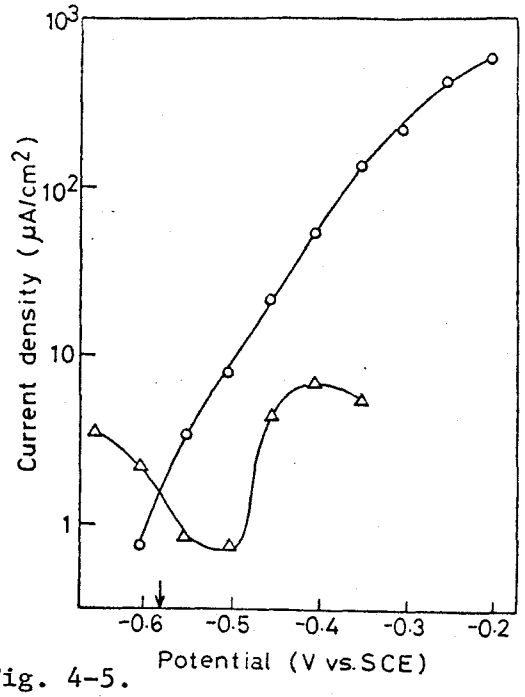

Fig. 4-5.
(o) Oxidation and (△) reduction curves of rutile obtained from Fig. 4-3

proceeded with a potential dependency in a normal fashion. No report has been published on the potential dependency of oxygen adsorption at rutile. However, it is quite normal for a neutral molecule to show a potential dependency of adsorption.[76] In Fig. 4-4 and 4-5, the author thinks that oxygen shows its maximum adsorption at the potential where the maximum current is observed.

Figure 4-6 shows polarization curves of the mildly dried rutile electrode with high N_D measured in 0.1 M $LiClO_4$-2-propanol. The curves showed similar tendency to those obtained in methanol shown in Fig. 4-2. Then, the same argument as that applied to methanol seems to be valid to 2-propanol. The cathodic current in the dark seemed to increase a little upon introduction of oxygen into the solution as is observed by comparing

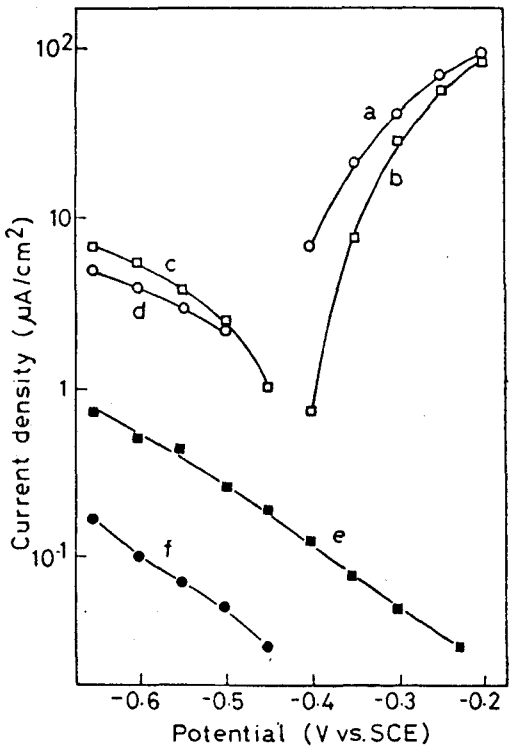

Fig. 4-6.

Polarization curves of the mildly dried rutile electrode with high N_D in 0.1 M $LiClO_4$-2-propanol. Notations are the same as in Fig. 4-2

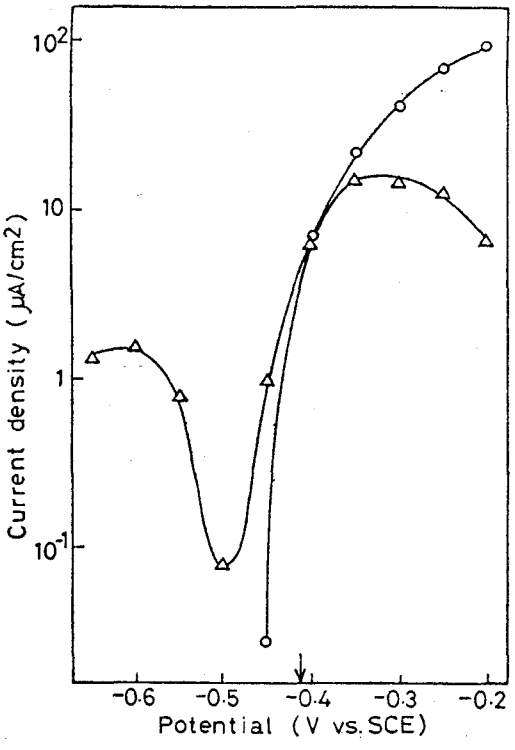

Fig. 4-7.

(○) Oxidation and (△) reduction curves of rutile obtained from Fig. 4-6

the curves (e) with (f), and this result was different from the case of methanol. This means that oxygen adsorbed without illumination. However, the oxygen adsorption in the dark is believed to have no serious role in the overall catalytic process, because the extent of the adsorption in the dark was very low compared with that under illumination, as is observed by comparing the curve (e) with (f). Figure 4-7 shows the anodic polarization curve of 2-propanol and the cathodic curve of oxygen obtained from Fig. 4-6 in the same manner as in the case of methanol. By comparing the anodic polarization curve in Fig. 4-7 with that in Fig. 4-4, it can be noticed that the oxidation current of 2-propanol was smaller than that of methanol at respective potentials. This is possibly brought about by the difference in the amount of adsorbed alcohol, as discussed in chapter 2.

(3) Effect of Surface Pre-treatment

The followings are noticed by comparing individual polarization curves in Fig. 4-4 with that in Fig. 4-5; (i) reduction current of oxygen was large and oxidation current of methanol was small at the mildly dried electrode, and (ii) the anodic oxidation of methanol commenced at a relatively less noble potential at thoroughly dried electrode than at mildly dried electrode. These phenomena must be connected to surface condition of the electrode.

It is believed that the rutile surface is usually covered with OH as well as water molecules, as already described in chapter 2.[29] However, when rutile was degassed at 300-350°C, surface water molecules are removed, leaving the rutile surface partially hydroxylated.[28] On the other hand, it was reported that surface OH was removed irreversibly when TiO_2 was heat treated above 450°C, and that the surface was not rehydrated even after it was contacted with an aqueous solution for 150 days.[31] The rutile single

crystal used in the present study was prepared at a very high temperature above the melting point of TiO_2. Then, the amount of irreversibly adsorbed surface OH seems to be rather low. Anyway, irreversibly adsorbed OH is believed not to be removed from the surface by prolonged drying at room temperature. The reversibly adsorbed OH must have brought about the above mentioned difference in the polarization behavior. The effects of the pre-treatment on the polarization curves were reproducible. For example, the polarization curves in Fig. 4-3 changed into those in Fig. 4-2 after rutile dried in the desiccator was held in an aqueous solution for about 1 week, and the reverse change was true if the electrode was held in the desiccator for 3 days. It follows from this discussion that the " thoroughly dried electrode" had a less amount of OH on the surface which was readily removable during drying.

It was already reported that the higher the degree of surface OH coverage was, the more oxygen adsorbed.[75,77] Present results on the cathodic polarization curve of oxygen was, therefore, in accord with these reports. The current value of the oxidation of methanol was higher at the thoroughly dried rutile electrode than at the mildly dried one, as already speculated in chapter 2 as well as by Stone et al..[10]

The potential at which the oxidation of methanol commenced was more cathodic at the thoroughly dried electrode than at mildly dried one. To search the origin of this behavior, Mott-Schottky plots of differential capacitance of the electrode with high N_D were made at 1 kHz in the dark. The results are shown in Fig. 4-8 for both cases of the thoroughly dried and mildly dried. The flat-band potential V_{fb} was found to shift to a less noble potential when the degree of surface OH coverage was decreased. The result in this figure, however, merely shows that V_{fb} shifted cathodically by the promotion of drying, since the plots of $1/C^2$ vs. V at a fixed

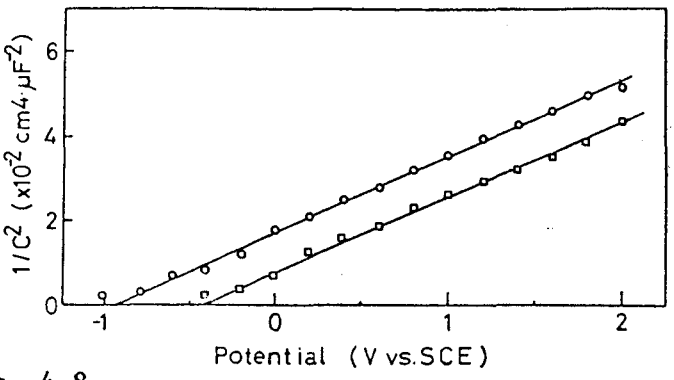

Fig. 4-8. Mott-Schottky plots of the rutile electrode in 0.1 M $LiClO_4$-CH_3OH saturated with O_2 at 1 kHz in the dark. This figure was obtained after rutile was pre-treated by different methods: (o) dried thoroughly in desiccator; (□) dried mildly by hot air.

frequency of 1 kHz do not give any decisive conclusion on an absolute value of V_{fb} as well as N_D.[60,61] Nevertheless, it is noticed that the oxidation of methanol commenced at around V_{fb} at both electrodes. It is quite reasonable for an oxidation reaction consuming positive holes to proceed at potentials anodic to V_{fb}. The flat-band potential of rutile was reported to shift regularly depending on pH of aqueous solutions.[23] This behavior is usually observed at oxide electrodes, and is believed to be due to dissociation of surface hydroxyl groups,[30] as described in chapter 2. The flat-band potential is represented by Eq. 4-3 [30]

$$V_{fb} = \text{const.} + \frac{RT}{2F} \ln \frac{a_{TiO^-}}{a_{Ti^+}} - \frac{2.3}{F} RT(pH) \qquad (4\text{-}3)$$

Removal of water from surface will lead no change in the ratio of a_{TiO^-}/a_{Ti^+}, bringing no shift of V_{fb} so long as the solution pH is held constant, since the electrode must lose the same amount of H^+ and OH^- in desorption of water. However, in the present study, a shift of V_{fb} was observed. If dissociation of surface OH takes place in a different extent at the electrodes having different surface coverage of OH, then, the shift should appear. However,

we have no definite information on this point. Although the interpretation of the shift in V_{fb} is ambiguous at present, it is evident that the phenomenon is connected to the adsorbed amount of methanol and OH.

(4) Reaction Rates

The rate of the photocatalytic reaction should be given by the current value at the intersection point of the oxidation curve of methanol and the reduction curve of oxygen in Figs. 4-4 and 4-5, as the same manner as discussed in chapter 3. However, in the present study, the oxidation and the reduction curves in Fig. 4-4 seemed to intersect with each other in a considerably wide range. Then, an another method is necessary to find out the intersection point. The catalyst must have a fixed potential when the photocatalytic reaction is proceeding under a steady state condition. This potential was obtained by measuring the open-circuit potential of the illuminated rutile catalyst in the methanol solution containing oxygen, and is shown on the potential axis of Fig. 4-4 with an arrow. In the case of Fig. 4-5, the measured potential of the catalyst was in good accordance with the intersection point. The rate of the photocatalytic reaction was, then, estimated as the current value at this potential.

The reaction rates are summarized in Table 4-1 together with the result obtained for the other rutile electrode with low N_D. Table 4-1 also contains the reaction rates obtained by the chemical analysis which was described in an above section. The reaction rates obtained by the chemical analysis roughly coincided with those by the electrochemical analysis. By this, validity of the electrochemical analysis could be demonstrated. A high reaction rate was obtained when the rutile catalyst had a large amount of adsorbed OH on it. This result qualitatively accords with other reports on the oxidation of 2-propanol.[10,68,70] The reaction rate for the

oxidation of 2-propanol is shown in Table 4-1. A low reaction rate of 2-propanol compared with that of methanol is possibly brought by the small amount of adsorbed 2-propanol, as stated in chapter 2.

(5) The Reaction Mechanism

If methanol as well as 2-propanol molecules are oxidized through by a chemical process, not by an electrochemical process, then no appreciable oxidation current of the alcohols would be appear at the potential where the reaction is proceeding. Therefore, any process in which alcohol molecules reacts chemically with some chemical species to give the reaction products needs to be modified.

Recently, Stone and his co-workers proposed a mechanism of oxygen reduction[69,75] and of oxidation of 2-propanol by oxygen[10,69] on illuminated rutile catalysts. They observed that oxygen adsorption took place when rutile was illuminated with the light having higher energy than its band gap and that the amount of adsorbed oxygen was large for rutile with high surface coverage of OH. Their results are qualitatively in accord with our present results. According to them, positive hole is trapped firstly by OH_s^- on the rutile surface.[10]

$$OH_s^- + p^+ \longrightarrow OH_s \cdot \quad \text{(trapping)} \qquad (4\text{-}4)$$

On the other hand, the conduction band electron reacts with oxygen to form O_2^-.[10]

$$O_2 + e^- \longrightarrow O_{2\ ad}^- \quad \text{(chemisorption)} \qquad (4\text{-}5)$$

These two processes were supported later by Cundall et al.[71] and fit well

in the experimental results obtained in this study.

As mentioned in an above section, an important point given by the present electrochemical analysis is that both the oxidation of 2-propanol and methanol proceeds through exchange of electronic carriers. The present study also confirmed that oxidation reaction was little influenced by the amount of adsorbed oxygen. These results suggest a mechanism that the foundamental steps of the alcohol oxidation and the oxygen reduction do not interfere with each other. Therefore, the mechanism for the oxidation of methanol is the " current doubling" process, which is the same as described in chapters 2 and 3. Inhibition of the " current doubling" process by oxygen was reported for the oxidation of formate dissolved in an aqueous solution on ZnO.[12] If $\dot{C}H_2OH$, which is produced by the oxidation of methanol by positive hole, combines preferentially with oxygen by a chemical reaction, the anodic photo-current of methanol should be decreased down to half the value when the atmosphere is switched from nitrogen to oxygen. However, at the potential shown with the arrow in Fig. 4-4, the decrease in the current upon introduction of oxygen into the solution was large compared with half the value of the current measured in nitrogen atmosphere. This result implys that the reduction of oxygen proceeds independenly on the oxidation process. Hence, the oxidation step do not change by introduction of oxygen.

If the view that the alcohol oxidation and oxygen reduction proceed without any interference with each other is realized, then, the reduction of oxygen may proceed in the followings;

$$O_{2\ ad}^{-} + H^{+} \longrightarrow HO_{2\ ad}^{\cdot} \qquad (4\text{-}6)$$

$$HO_{2\ ad}^{\cdot} + e^{-} \longrightarrow HO_{2\ ad}^{-} \qquad (4\text{-}7)$$

$$HO_{2\ ad}^{-} + H^{+} \longrightarrow H_2O_2 \qquad (4\text{-}8)$$

These sequence of the reactions have been accepted widely in the electrochemical field as the reaction mechanism of oxygen to hydrogen peroxide.[78] In the case of water production, a part of hydrogen peroxide produced would decompose into water.

$$H_2O_2 + 2\,H^{+} + 2\,e^{-} \longrightarrow 2\,H_2O \qquad (4\text{-}9)$$

In addition, the following reaction proposed by Stone and Bickley[75] may proceed instead of Eq. 4-7.

$$HO_{2\ ad}^{\cdot} + OH_{s}^{-} \longrightarrow H_2O + O_{2\ ad}^{-} \qquad (4\text{-}10)$$

However, the author does not intend here to claim that the reduction mechanism is represented in the above equations. The important thing is to establish a mechanism in which the alcohol and oxygen molecules are oxidized and reduced, respectively, through the individual electronic exchange under a condition that the catalyst maintains electrical neutrality.

CHAPTER 5

THE DEVELOPMENT OF PHOTO-ELECTROCHEMICAL CELLS FROM SYSTEMS WITH PHOTOCATALYTIC REACTIONS

5-1 INTRODUCTION

In chapters 3 and 4, photocatalytic reactions on rutile were investigated mainly by electrochemical method based on the local cell process. In the systems of methanol-quinones and alcohol-oxygen which were described in chapters 3 and 4, respectively, as well as in the system reported before,[42] alcohol was oxidized through the " current doubling" process to corresponding aldehyde or ketone with the same rate that either one of quinone, oxygen or methylene blue[42] was reduced by the condution band electrons in rutile. The anode process was distinctly influenced by the illumination on rutile, while the cathode process was not. In the former process, " photo-sensitized electrolytic oxidation" [6] was observed, that is, the oxidation proceeds at a less noble potential than that expected by thermodynamics, while the latter process was obeyed in accordance with usual thermodynamics, as shematically shown in Fig. 5-1. Therefore, the behavior of the cathode process of the local cell of the photocatalytic reaction is thought to be eventually the same as that on a metal surface. Then, if such a local cell is realized on illuminated rutile, one can in principle separate the local cell into individual reactions in such a way that the " photo-sensitized oxidation" process proceeds at an illuminated

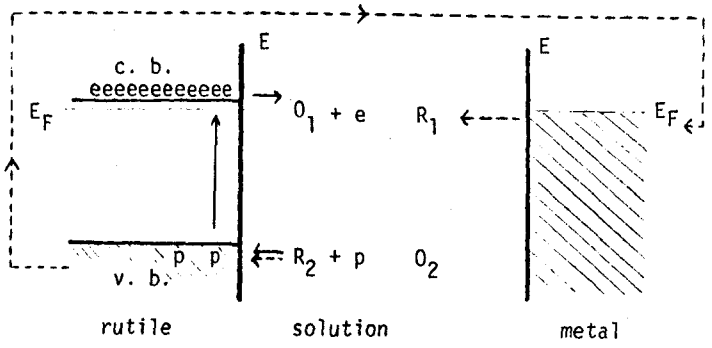

Fig. 5-1. Schematic diagram of photocatalytic reaction and photo-electrochemical cell reaction.
Path of electrons; —— catalytic reaction
---- cell reaction

rutile anode of the " photo-electrochemical cell" [7] and that conventional reduction process at a metal cathode.

In this chapter, some photocatalytic reactions on rutile are developed into photo-electrochemical cells. The quantum yield and the energy efficiency of the cells are obtained.

5-2 EXPERIMENTAL

A rutile electrode and a Pt electrode were prepared by the same manner as described in chapters 2 and 3, respectively. The (111) face of a p-type GaP wafer was used as a p-type semiconductor electrode and the back face of the crystal was coated with an In-Zn alloy at about 500°C to obtain an ohmic contact. Before measurements, the rutile and the GaP electrode were dipped in conc. nitric acid and conc. hydrochloric acid for 1 min, respectively. Then, they were washed by de-ionized water for about 30 min and dried by hot air.

The solutions used in this study were methanol, water and 2-propanol. $LiClO_4$ or gaseous hydrogen chloride was dissolved in these solutions as the supporting electrolyte. Nitrogen or oxygen gas was bubbled into the

solution before measurements for about 30 min.

The semiconductor electrodes were illuminated by a 500 W ultra-high pressure mercury arc lamp and the light of wave length shorter than 350 nm was cut off by setting a convex glass lens in front of a quartz window of the measurement cell. When methylene blue was dissolved in the solution, a $CuSO_4$ solution filter was set in front of the cell window to prevent the photo-excitation.[79)]

Hydrogen gas produced by the cell reaction was detected by gas chromatography.

Other details have been given before.

5-3 RESULTS AND DISCUSSION

(1) Development of Photocatalytic Reactions on Rutile into Photo-cell

Figure 5-2 shows polarization curves of a rutile electrode in 10^{-1} M HCl-methanol containing 10^{-4} M methylene blue. The measured cathodic

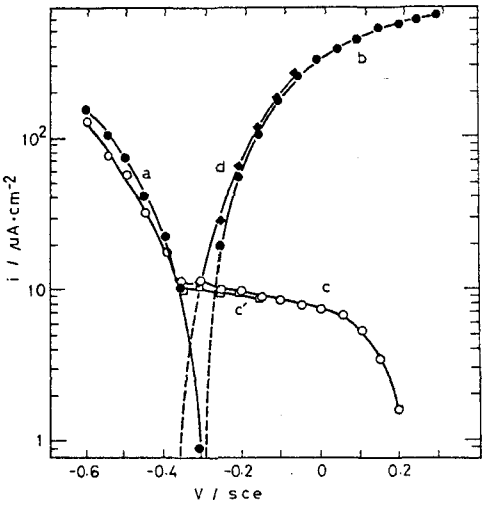

Fig. 5-2. Polarization curves of a rutile electrode in 0.1 N HCl–CH_3OH containing 10^{-4} M methylene blue: (a) measured cathodic curve under illumination; (b) measured anodic curve under illumination; (c) measured cathodic curve in the dark; (c') real cathodic curve and (d) real anodic curve.

polarization curve (a) and anodic curve (b) were obtained under illumination. The cathodic curve (c) was obtained in the dark. The cathodic current increased exponentially with increasing polarization in the potential less noble than -0.35 V. Hence these cathodic curves are presumably connected with electrons in the conduction band.[2,3] The anodic curve (b) was connected with positive holes in the valence band of rutile. The real anodic curve (d), oxidation of methanol, was obtained as the sum of the current in the curve (b) and absolute value of the current in the curve (c), and subtraction of the curve (a) from the (c). The real cathodic curve (c'), reduction of methylene blue, was obtained from the curve (c) by subtraction of a residual current of unknown nature which was obtained in 0.1 M HCl-methanol. The actual rate of the photocatalytic reaction corresponds to the current which is obtained as the intersection point of the curves (d) and (c').[42] It was already clarified that the actual rate of the photocatalytic reduction of methylene blue could be determined by this electrochemical analysis.[42] Although the shapes of various polarization curves seem to be different from those reported previously, it is mainly due to different illumination intensity and different concentration of methylene blue.[42] In anyway, this figure indicates that oxidation of methanol to formaldehyde and reduction of methylene blue to leuco-methylene blue proceed simultaneously on the illuminated rutile electrode, as reported before.[42]

If two rutile electrodes were immersed in the same solution and one rutile is illuminated and the other is not, a photo-electrochemical cell is formed and the performance will be characterized by the curves (b) and (c) in Fig. 5-2. The photo-electrochemical cell almost the predicted performance was obtained.

If the rutile electrode in the dark is replaced by an insoluble metal

electrode, a curve similar to (c) will be obtained. Hence, it will be possible to construct a photo-electrochemical cell using illuminated rutile as the anode and a metal electrode as the cathode. Figure 5-3 gives polarization curves of the illuminated rutile and a Pt electrode in the same solution as in Fig. 5-2. The measured cathodic polarization curve (c) of the Pt electrode in Fig. 5-3 is analogous in shape to the curve (c) of the rutile electrode in Fig. 5-2. However, when the Pt cathode is highly polarized within the potential region of the cell operation, hydrogen evolution seems to occure, superposed on a diffusion limiting reduction of methylene blue. Then, the Pt cathode was replaced by a Hg-pool electrode to prevent the cathodic hydrogen evolution. Figure 5-4 shows the polarization curves of the rutile and the Hg-pool electrode. The curve (c') shows the true reduction current of methylene blue. A photo-electrochemical cell was obtained, when the cell was operated under short-circuit condition and Faraday's low was well established with respect to methylene blue. Thus, the same reaction as the local cell process on rutile catalyst[42] could be developed into a photo-electrochemical cell.

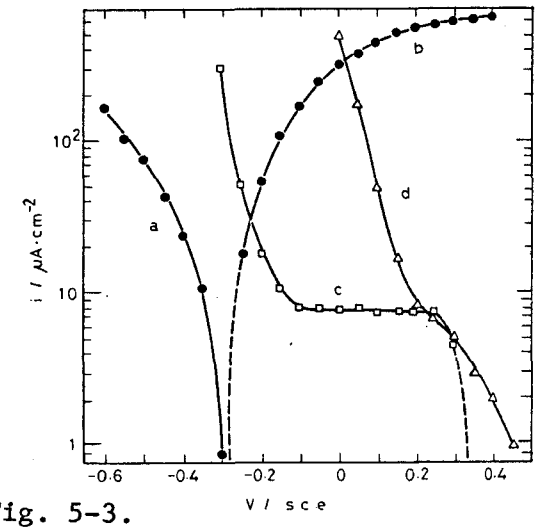

Fig. 5-3.
Polarization curves of the illuminated rutile, a Pt and an illuminated GaP electrode in 0.1 N HCl–CH_3OH containing 10^{-4} M methylene blue: (a) cathodic curve at rutile; (b) anodic curve at rutile; (c) cathodic curve at Pt; (d) cathodic curve at GaP.

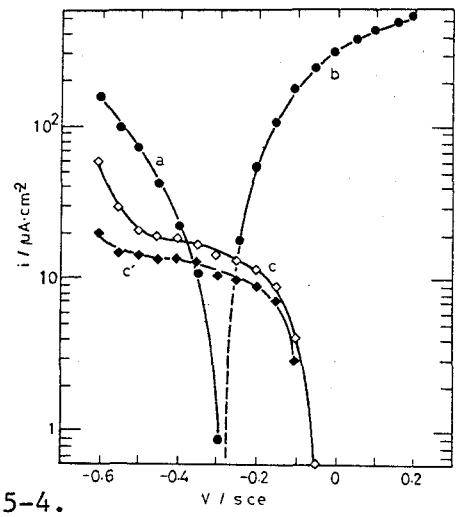

Fig. 5-4.
Polarization curves of the illuminated rutile and a Hg-pool electrode in 0.1 N HCl–CH_3OH containing 10^{-4} M methylene blue: (a) cathodic curve at rutile; (b) anodic curve at rutile; (c) cathodic curve at Hg and (c') real cathodic curve at Hg.

rutile anode: $CH_3OH + p^+ \longrightarrow HCHO + 2H^+ + e^-$ (5-1)

Hg cathode: $M^+ + 3H^+ + 2e^- \longrightarrow MH_3^{2+}$ (5-2)

where M represents the uncharged center of the methylene blue molecule.

When the Hg-pool electrode was replaced by an illuminated p-GaP semiconductor electrode, the cell performance was improved as expected from the case of the electrochemical photolysis of water,[7,9] which is also shown in Fig. 5-3 as the curve (d). However, in this case, the hydrogen evolution reaction seemed to occure in preference to the reduction of methylene blue.

(2) Some Photo-cells Constructed

The curves (c) in Figs 5-3 and 5-4 show that hydrogen evolution preferentially occurred when the cathode is highly polarized except for a Hg cathode. A photo-electrochemical cell which has a Pt cathode can then produce hydrogen instead of reducing methylene blue. The measured polarization curve of the Pt electrode in 0.1 M HCl-methanol is shown in Fig. 5-5

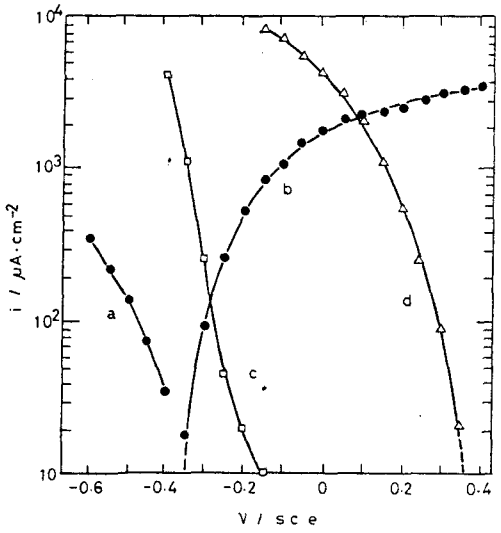

Fig. 5-5. Polarization curves of the illuminated rutile, the Pt and the illuminated GaP electrode in 0.1 N HCl-CH_3OH. Notations are the same as in Fig. 5-3

together with the polarization curves of the illuminated rutile electrode. When the Pt electrode was again replaced with the illuminated GaP electrode, the cell performance was improved as expected, which is shown in Fig. 5-5 as the curve (d). The difference in performance of the GaP electrode between Figs. 5-3 and 5-5 was due to a difference in the illumination intensity. In practice, a photo-electrochemical cell was constructed of the Pt and the illuminated rutile electrode in 0.1 M HCl-methanol. And after a cell operation under a short-circuit condition for more than 20 hr, hydrogen gas and formaldehyde were detected as the products of the cell reaction.

In chapter 4, it was clarified that a photocatalytic oxidation of alcohol by oxygen on rutile proceeds by the local cell process. Therefore, a photo-electrochemical cell would be constructed in 0.1 M $LiClO_4$-methanol saturated with oxygen as the same manner as just described. Fig. 5-6 shows polarization curves of the cell:

illuminated rutile | 0.1 M $LiClO_4$ • CH_3OH, O_2 | Pt or illuminated GaP

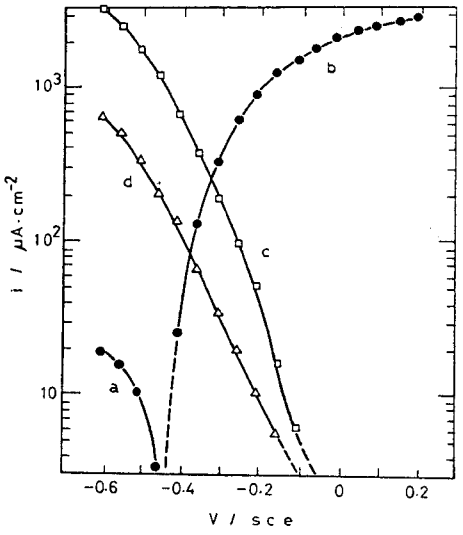

Fig. 5-6. Polarization curves of the illuminated rutile, the Pt and the illuminated GaP electrode in 0.1 M $LiClO_4$–CH_3OH saturated with O_2. Notations are the same as in Fig. 5-3

Two kinds of cells, which contain oxygen or proton as the cathode active material, were also constructed using 2-propanol as the same manner as that using methanol. The characteristics of the cells were analogous to those using methanol, although their performance were poorer. These results were in accord with those for the photocatalytic reaction of 2-propanol containing oxygen on illuminated rutile, as described in chapter 4, that is, the reaction behavior was similar to that of methanol-oxygen system but the reaction rate was lower. Acetone was detected as the product for the cell reaction, which is the same one as in the case of the photocatalytic reaction.[71]

(3) The Quantum yield and the Energy Efficiency

Typical quantum yield and energy efficiency of the three cells were shown in Table 5-1. The values were obtained at the maximum output power of the cell. The quantum yield of rutile Φ which is illuminated by 400 nm monoclomatic light is defined as $\Phi = i_{ph}/n_{ph}$, where i_{ph} is the number of electrons flowed as a photo-current per cm^2 per hr, and n_{ph} is the number of photons incident upon the unit electrode surface area in unit time, which was determined in the same manner as reported[80] (8.1×10^{17} photons/cm^2•h). The energy efficiency is defined as η_1 and η_2. η_1, which relates to the output power of the cell, is determined as $\eta_1 = W_{cell}/W_{ph}$, where W_{cell} is the output power of the cell and W_{ph} is the energy incident upon the unit electrode surface per second (1.2 W/cm^2). η_2, which relates to the stored

Table 5-1. Quantum yield and energy efficiency

Electrode	Electrolyte	Product	Quantum yield* Φ	Energy efficiency† η_1	η_2	Condition Potential of rutile (*sce*)
Rutile-Pt	0.1 N HCl-CH_3OH	HCHO, H_2	4.0×10^{-3}	2.8×10^{-6}	1.6×10^{-5}	−0.33
Rutile-Pt	0.1 M $LiClO_4$-CH_3OH saturated with O_2	HCHO, H_2O_2	7.7×10^{-3}	1.0×10^{-5}	-3.6×10^{-5}	−0.37
Rutile-Pt	0.1 N HCl-$(CH_3)_2CHOH$	CH_3COCH_3, H_2	3.7×10^{-3}	8.3×10^{-7}	1.4×10^{-6}	−0.25

* 400 nm monoclomatic light, intensity: 8.1×10^{17} photons/cm^2 per h.
† Intensity of light; 1.2 W/cm^2.

enthalpy of chemical substances, is expressed as $\eta_2 = (W_f - W_i)/W_{ph}$, where W_f is the sum of the enthalpy of the reacton products in the cell and W_i is the sum of the enthalpy of the reactants for the same cell. These values were calculated based on the observed quantity of electricity at the maximum output power of the cell.

To compare the quantum yield for the cell of methanol photolysis with that for the cell of water photolysis, the quantum yields in 0.1 M HCl-methanol and in 0.1 M HCl-water were plotted as a function of the potential of the rutile electrode (Fig. 5-7). Similar tendency as reported by Ohnishi et al. were obtained.[81] The quantum yield for the cell of methanol was larger than that for the cell of water, as shown in Fig. 5-7. The flat-band potentials and the donner densities of the rutile electrode measured in both solutions gave the same values. Therefore, this tendency was probably brought due to the " current doubling" effect for the methanol oxidation.

The obtained values of the quantum yield and the energy efficiency for these cells were rather low. However, recent publications showed that the quantum yield on rutile electrodes[57,81] and on a CdS electrode[58] varies distinctly depending on various factors, such as band bending, carrier

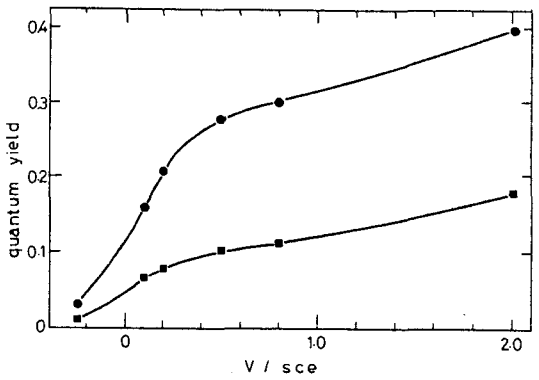

Fig. 5-7. Quantum yield *vs* potential for a rutile electrode. Solution; ● 0.1 N HCl-CH_3OH, ■ 0.1 N HCl-H_2O. The illuminated light intensity; 1.9×10^{17} photons/cm^2 per h. 400 nm monoclomatic light.

density of an electrode, wave length and intensity of illuminating light, reflection of light at an electrode surface and light absorption in the electrolyte. Therefore, the values in Table 5-1 and Fig. 5-7 give only some indications of the approximate quantum yield and energy efficiency of the systems.

CHAPTER 6

CORRELATION BETWEEN PHOTO-ELECTROCHEMICAL CELL REACTIONS AND PHOTOCATALYTIC REACTIONS ON RUTILE

6-1 INTRODUCTION

When a photocatalytic reaction based on the local cell on rutile is established, a photo-electrochemical cell can be constructed, as demonstrated in chapter 5.

If one chooses an oxidizing agent whose redox-potential is more noble than the potential at which the oxidation of water commences on an illuminated rutile electrode, then, he can easily construct a photo-electrochemical cell by using a rutile anode and a Pt cathode. The performance of the cell will be different depending on redox-potentials of the oxidizing agents chosen so long as the anodic process is not heavily disturbed by the existence of the oxidizing agent, which may bring a partial cathodic current.

If the Pt cathode is taken out from the cell, and the rutile electrode is illuminated at the open-circuit condition, then, a local cell must be established on the illuminated rutile surface with the same reaction as that of the photo-electrochemical cell. The reaction in this case may be termed as an photocatalytic reaction, as in the cases of reduction of quinones and oxygen on illuminated rutile in methanol solutions described in chapters 3 and 4, respectively. It is quite natural to expect, however, that reaction

behaviors will be different between in the photo-electrochemical cell and photocatalytic process.

The purpose of this chapter is to present the difference in the behaviors between the two kind of reactions by using several kind of oxidizing agents.

6-2 EXPERIMENTAL

A rutile electrode, a Pt electrode and rutile powder catalyst were prepared by the same manner as described in chapters 2 and 3.

A solution used in this study was 0.5 M H_2SO_4 containing an oxidizing agent. Oxidizing agents chosen were $KMnO_4$, $K_2Cr_2O_7$ and $Fe_2(SO_4)_3$. Water used as the solvent was distilled twice and the H_2SO_4 solution was pre-electrolyzed for 48 hr. All chemicals used were of guaranteed reagent grade. Nitrogen gas was bubbled into the solution during all the electrochemical and chemical experiments. In the case of the experiment using $KMnO_4$ solution, a $CoSO_4$ solution filter was set in front of the cell window to prevent the photo-excitation of MnO_4^-.[79] The concentration of chemical species in the solution was determined by means of absorptiometry.

Other details such as a light sourse, construction of an electrolytic cell and method of polarization measurements were described in chapters 2 and 3.

6-3 RESULTS AND DISCUSSION

(1) Photo-electrochemical Cells

Figure 6-1 shows polarization curves of photo-electrochemical cells of

$$\text{rutile} \;\big|\; 0.5\ \text{M}\ H_2SO_4 \;\big\vert\; \text{Ox},\ 0.5\ \text{M}\ H_2SO_4 \;\big|\; \text{Pt}$$

where Ox denotes an oxidizing agent. This figure suggests that if the cell of

$$\text{rutile} \;\big|\; \text{Ox},\ 0.5\,\text{M}\ H_2SO_4 \;\big|\; \text{Pt}$$

works ideally, the cell reaction is composed of the oxidation of water and the reduction of the oxidizing agent, respectively. The term " ideally" means that the partial cathodic reduction of Ox and the oxidation of the product formed at the Pt cathode are negligible at the rutile electrode. Establishment of this ideal condition was confirmed at least in the case of the reduction of MnO_4^- to MnO_2 and of $Cr_2O_7^{2-}$ to Cr^{3+}, by analyzing the concentration of the oxidizing agent in the cell as a function of the quantity of electricity drawn in a short-circuit condition.

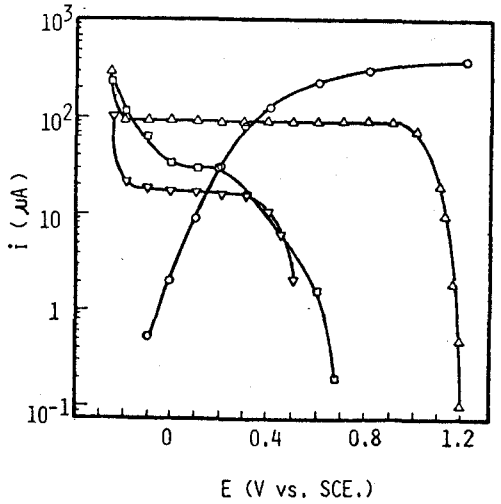

Fig. 6-1. Polarization curves of the illuminated rutile and the Pt electrodes in 0.5 M H_2SO_4 with and without 5×10^{-4} M oxidizing agent. (○) Anodic curve at rutile without oxidizing agent, and cathodic curves at Pt with (△) $KMnO_4$, (□) $K_2Cr_2O_7$. and (▽) $Fe_2(SO_4)_3$.

(2) Photocatalytic Reactions

Chemical analysis: When a rutile powder catalyst was suspended in 0.5 M H_2SO_4 solution (50 cm^3) containing an oxidizing agent, the concentration of the oxidizing agent was decreased by the illumination. The result is shown in Fig. 6-2.

The solutions retained their original absorbance if they are illuminated without the rutile catalyst for 20 hr. By the reaction, the solution containing $KMnO_4$ produced a brown precipitate and the purple solution turned light yellow. The other solutions became transparent and no deposit was detected on the catalyst. Accordingly, the cathodic process of the photocatalytic reactions are reduction of MnO_4^-, $Cr_2O_7^{2-}$ and Fe^{3+} to MnO_2, Cr^{3+} and Fe^{2+}, respectively. On the other hand, the anodic process is oxidation of water.[6] These results suggest that illuminated rutile worked effectively as the catalyst, bringing the same reaction as in the photoelectrochemical cell.

The reaction in Fig. 6-2 seems to be the first order with respect to

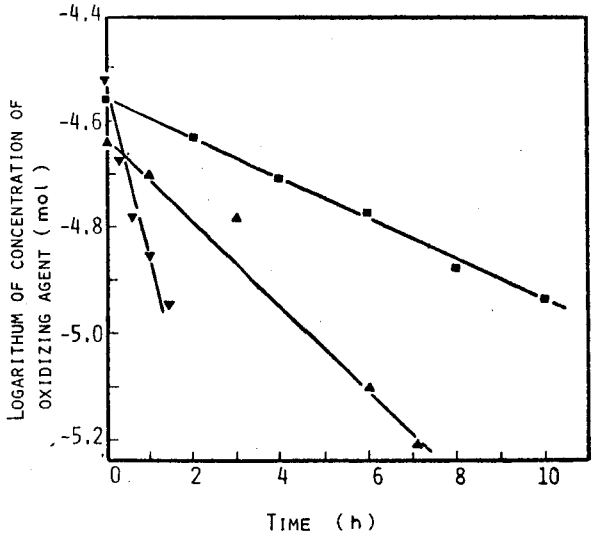

Fig. 6-2. Change of the concentration of oxidizing agents in 0.5 M H_2SO_4 with the reaction time on the illuminated rutile powder catalyst. The solutions containing (▼) Fe^{3+}, (■) $1/2 \cdot Cr_2O_7^{2-}$, and (▲) MnO_4^-, respectively.

Table 6-1. Reaction rates determined by electrochemical analysis and reaction rate constants determined by chemical analysis

Solution	$K_2Cr_2O_7$	$KMnO_4$	$Fe_2(SO_4)_3$
Electrochemical analysis (μA)	0.26	0.73	2.2
Chemical analysis ($\times 10^{-4}$ 1/s)	1.1	1.5	6.0

the oxidizing agent chosen, since linear relations were established between logarithm of the concentration of the oxidizing agent and the reaction time. The rate constants calculated from the slope of the lines are summarized in Table 6-1.

Electrochemical analysis: Fig. 6-3 shows the oxidation curve of water by positive holes and the reduction curves of the oxidizing agents by the conduction band electrons on rutile. They were obtained by the same manner as described in chapter 3 by analyzing the polarization curves obtained under various conditions.

The reaction rates: The rates of the photocatalytic reactions were, then, possible to be determined as the current values of the intersection points in Fig. 6-3, as the same manner as described in chapter 3. In the cases of MnO_4^- and $Cr_2O_7^{2-}$, three and six Faradays are needed to produce 1 mole of MnO_2 and 2 moles of Cr^{3+}, respectively. One-third of the current values at the intersection points in Fig. 6-3, thus, correspond to the reaction rates for these systems. The reaction rates estimated from the electrochemical measurements are summarized in Table 6-1 together with the reaction rate constants determined by the chemical analysis which was described above.

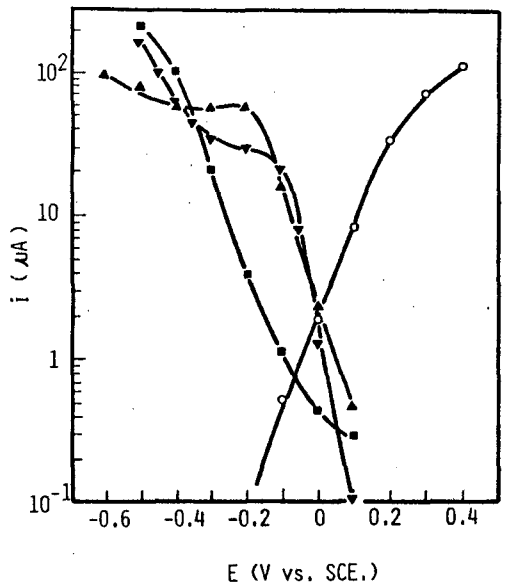

Fig. 6-3. Polarization curves of the rutile electrode in 0.5 M H_2SO_4 with and without the oxidizing agent. (○) Anodic curve without the oxidizing agent under illumination. Cathodic curves with 5×10^{-4} M (▲) $KMnO_4$, and 2.5×10^{-4} M (▼) $Fe_2(SO_4)_3$ and (■) $K_2Cr_2O_7$ in the dark.

The value of the reaction rate on the illuminated rutile catalyst is determined by feasibility of electron exchange between the semiconductor and the species in the solution, as discussed in chapter 3 for the case of quinones dissolved in methanol. The feasibility is determined by the relative position of the energy levels of the band edges of semiconductor to electron energy of the chemical species which are distributed with specified rearrangement energy.[3,5] Accordingly, the difference in the reaction rates of oxidizing agents in Table 6-1 seems to be due to this factor. Detailed discussion about the difference in the reactivity could not be done, since we have no data for the rearrangement energy of MnO_4^- and $Cr_2O_7^{2-}$ which are reduced by three step process.

(3) Difference in Behaviors of Cathodic Polarization Curves between the Photo-emf Cells and Photocatalytic Reactions

It is noticed by comparing Figs. 6-1 with 6-3 that main difference lies in cathodic polarization behaviors of the oxidizing agents.

Cathodic curves on the rutile electrode given in Fig. 6-3 commenced at almost the same potential of 0.1 V vs. S.C.E.. This means that the over-potential was different depending on the kind of the oxidizing agents. In the case of a semiconductor electrode, externally applied potential causes a change of band bending in the semiconductor.[2-5] When the semiconductor electrode is polarized at potentials anodic to the flat-band potential V_{fb}, the bands bend up toward the surface.[2-5] Consequently, the cathodic current should be controlled by this energy barrier, and eventually independent of the redox-potentials of the oxidizing agents used as long as the cathodic process is affected only by the electron density at the semiconductor surface. Validity of this view was already reported on ZnO.[46] In that case, the potential barrier to bring the cathodic current flow of an order of 0.1 $\mu A/cm^2$ was 0.6 eV at the highest case.[46] Therefore, the cathodic polarization curves in Fig. 6-3 are judged to be reasonable, since V_{fb} of rutile in 0.5 M H_2SO_4 are considered to be -0.1 V vs. S.C.E..[61]

On the other hand, polarization of the rutile electrode at a potential cathodic to V_{fb} brings the energy barrier for the positive holes to reach the electrode surface in the same manner as electrons for the anodic polarization.[3,5]

When both electrons and positive holes transfer from the electrode to chemical species in the solution, as is the case of the present photo-catalytic reaction, the flat-band condition will be feasible for the transfer of the both carriers. The potential where the reaction proceeds

reflects this situation and locates around V_{fb}, as Fig. 6-3 shows. In this condition, the quantum yield of the reaction should be quite low, since electron-hole recombination predominates,[57,81] and the reaction rate is low as shown in Fig. 6-3. Therefore, it can be confirmed in the present study that good utilization of light energy will not be expected for the photocatalyst where the both bands participate in the reaction.

In the case of photo-electrochemical cells using the illuminated rutile anode and the metal cathode, it is necessary to take into consideration of the energy barrier only for positive holes in the anode. When the energy bands bend up enough to accelerate positive holes effectively to the semiconductor surface, a larger reaction rate can be expected than that of the photocatalytic reaction.

CHAPTER 7

CONCLUSION

The works in this thesis were carried out to investigate photocatalytic reactions on rutile by electrochemical measurements. The results obtained are summarized as follows.

1) The " current doubling" process has been found to proceed for the oxidation of methanol, ethanol and 2-propanol on an illuminated rutile electrode when the alcohol concentration in water is high. Number of $-Ti^{+}$ sites of rutile seems to play an important role in the reaction.

2) Photocatalytic reactions of quinones dissolved in methanol were investigated by employing electrochemical measurements based on the local cell process. It has been found that quinones are reduced by electrons in the conduction band of rutile to hydroquinone and that methanol is oxidized through the " current doubling" process to formaldehyde. The higher reaction rate was obtained for a quinone with a noble redox-potential. Photocatalytic oxidation of methanol and 2-propanol were studied by the similar manner to that in the case of quinones. It has been found that alcohol and oxygen are oxidized and reduced, respectively, via exchange of electronic carriers between the rutile catalyst and the chemical species. By these investigations, usefulness of the electrochemical method in analyzing photocatalytic reactions has been confirmed.

3) Correlation between photocatalytic reactions on rutile and photo-electrochemical cell reactions on a rutile anode and a metal cathode has been clarified. These reactions are composed of the " photo-sensitized electrolytic oxidation" and reduction which obeys usual thermodynamics.

4) The rates of some photocatalytic reactions on rutile which proceed by the local cell process are concluded to be, in general, lower than that of corresponding reactions at photo-electrochemical cells.

ACKNOWLEDGEMENT

The author would like to express his deep gratitude to Professor Hideo Tamura at Faculty of Engineering, Osaka University for his guidance and encouragement during the course of this investigation.

The author is indebted to Associate Professor Hiroshi Yoneyama for his warharted inspirous and many helpful discussions.

The author is also grateful to Dr. Chiaki Iwakura, Mr. Osamu Ikeda and Professor Yoshiharu Matsuda for their useful suggestions and discussions.

It is a real pleasure to express the author's thanks to all the members of Tamura laboratory for their friednships.

Finally, great many thanks are given to the author's parents for their understanding and encouragement.

REFERENCES

1) W. H. Brattain and C. G. Garrett, Bell System Tech. J., 34, 129 (1955).

2) V. A. Myamlin and Y. V. Plescov, " Electrochemistry of Semiconducors", p. 1, Plenum Press, New York (1967).

3) H. Gerischer, " Advance in Electrochemistry and Electrochemical Engineering", Vol. 1, p. 139 (Edited by P. Delahay), Interscience, New York (1961).

4) H. Gerischer, " Physical Chemistry", Vol. IXA, p. 463 (Edited by H. Eyring et al.), Academic Press, New York (1970).

5) A. K. Vijh, " Electrochemistry of Metals and Semiconductors", p. 1, Marcel Dekker, New York (1973).

6) A. Fujishima, K. Honda and S. Kikuchi, Kogyo Kagaku Zasshi, 72, 108 (1969).

7) A. Fujishima and K. Honda, Nature, 238, 37 (1972).

8) T. Freund and W. P. Gomes, " Catalysis Reviews", Vol. 3, p. 1 (Edited by H. Heinemann), Marcel Dekker, New York (1969).

9) H. Yoneyama, H. Sakamoto and H. Tamura, Electrochim. Acta, 20, 341 (1975).

10) R. I. Bickley, G. Munuera and F. S. Stone, J. Catal., 31, 398 (1973).

11) V. N. Filimonov, Dokl. Acad. Nauk. USSR, 154, 922 (1967).

12) S. R. Morrison and T. Freund, J. Chem. Phys., 47, 1543 (1967).

13) H. Gerischer, Surface Sci., 14, 97 (1969).

14) W. P. Gomes, T. Freund and S. R. Morrison, ibid., 13, 201 (1968).

15) H. Gerischer and H. Rösler, Chem. Ing. Tech., 42, 176 (1970).

16) R. Memming and F. Möllers, Ber. Bunsenges. Phys. Chem., 76, 609 (1972).

17) R. Memming, J. Electrochem. Soc., 116, 785 (1969).

18) Y. Takami, " Shyokubai Kogaku Koza", Vol. 5, p. 231 (Edited by Y. Ogino), Chizin-shyokan, Tokyo (1965).

19) H. Yoneyama and H. Tamura, Bull. Chem. Soc. Japan, 45, 3048 (1972).

20) G. D. Snell, " Colorimetric Methods of Analysis", 3rd ed., Vol. 3, p. 253, D. Van. Nostland (1950).

21) W. P. Gomes, T. Freund and S. R. Morrison, J. Electrochem. Soc., 115, 818 (1968).

22) K. W. Egger and A. T. Cocks, Helv. Chim. Acta, 56, 1516 (1973).

23) T. Watanabe, A. Fujishima and K. Honda, Chem. Lett., 897 (1974).

24) R. A. L. Vanden Berghe and W. P. Gomes, Ber. Bunsenges. Phys. Chem., 76, 481 (1972).

25) G. D. Parfitt and I. J. Wiltshire, J. Phys. Chem., 68, 3545 (1964).

26) V. Yu. Borovkov and V. B. Kazanskii, Kinetika i Kataliz, 15, 705 (1974).

27) S. Seki et al., " Kagaku Binran", p. 999, Maruzen, Tokyo (1975).

28) G. Munuera and F. S. Stone, Discuss. Faraday Soc., 52, 205 (1971).

29) H. P. Boehm, " Advance in Catalysis", p. 149, Academic Press, New York (1966).

30) F. Lohmann, Ber. Bunsenges. Phys. Chem., 70, 428 (1966).

31) Y. G. Bĕrubĕ and P. L. De Bruyn, J. Colloid Interface Sci., 27, 305 (1968).

32) J. F. Llopis, I. M. Tordesillas and F. Colom, " Encyclopedia of Electrochemistry of the Elements", Vol. VI, pp. 208-213, Marcel Dekker, New York (1976).

33) R. I. Bickley and K. M. Jayanty, Discuss. Faraday Soc., 58, 194 (1974).

34) K. Micka and H. Gerischer, J. Electroanal. Chem., 38, 397 (1972).

35) Y. G. Bèrubè and P. L. De Bruyn, J. Colloid Interface Sci., 28, 92 (1968).

36) M. Gleria and R. Memming, J. Electroanal. Chem., 65, 163 (1975).

37) F. F. Vol'kenstein, " Advance in Catalysis", Vol. 12, p. 189 (Edited by D. D. Eley et al.), Academic Press, New York (1960).

38) F. F. Vol'kenstein, ibid., Vol. 23, p. 157 (1973).

39) V. J. Lee, J. Chem. Phys., 55, 2905 (1971).

40) S. R. Morrison, J. Catal., 20, 110 (1971).

41) F. Garcia-Moliner, " Catalysis Reviews", Vol. 2, p. 3 (Edited by H. Heinemann), Marcel Dekker, New York (1969).

42) H. Yoneyama, Y. Toyoguchi and H. Tamura, J. Phys. Chem., 76, 3460 (1972).

43) H. Gerischer, Z. Phys. Chem. (N. F.), 26, 223 (1960).

44) H. Gerischer, ibid., 26, 325 (1960).

45) H. Gerischer, ibid., 27, 48 (1961).

46) S. R. Morrison, Surface Sci., 15, 363 (1969).

47) W. P. Gomes and F. Cardon, Z. Phys. Chem. (N. F.), 86, 330 (1973).

48) S. N. Frank and A. J. Bard, J. Amer. Chem. Soc., 97, 7427 (1975).

49) K. M. Sancier, J. Catal., 5, 314 (1966).

50) G. D. Snell, " Colorimetric Methods of Analysis", 3rd ed., Vol. 3, p. 305, D. Van Nostland (1950).

51) R. H. Bube, " Physical Chemistry", Vol. X, p. 515 (Edited by H. Eyring et al.), Academic Press, New York, (1970).

52) D. C. Coronemeyer, Phys. Rev., 87, 876 (1952).

53) M. Cordona and G. Harbeke, ibid., 137A, 1467 (1965).

54) R. G. Breckenridge and W. R. Hosler, ibid., 91, 793 (1953).

55) H. P. R. Frederikse, J. Appl. Phys. Suppl., 32, 2211 (1961).

56) M. Haradome, " Handotai Busseikogaku no Kiso", pp. 133-139, Kogyochosakai, Tokyo (1967).

57) H. Tamura, H. Yoneyama, C. Iwakura, H. Sakamoto and S. Murakami, J. Electroanal. Chem., in press.

58) H. Gerischer, ibid., 58, 263 (1975).

59) M. E. Peover, " Electroanalytical Chemistry", Vol. 2, p. 8 (Edited by A. J. Bard), Marcel Dekker, New York (1967).

60) E. C. Dutoit, R. L. Van Meirhaeghe, F. Cardon and W. P. Gomes, Ber. Bunsenges. Phys. Chem., 79, 1206 (1975).

61) E. C. Dutoit, F. Cardon and W. P. Gomes, ibid., 80, 475 (1976).

62) A. K. Ghosh, F. G. Wakim and R. R. Addiss, Phys. Rev., 184, 979 (1969).

63) R. Memming and F. Möllers, Ber. Bunsenges. Phys. Chem., 76, 475 (1972).

64) R. A. L. Vanden Berghe, F. Cardon and W. P. Gomes, Surface Sci., 39, 368 (1973).

65) M. C. Markham, M. C. Hannan and S. W. Evans, J. Amer. Chem. Soc., 76, 820 (1954).

66) M. C. Markham, M. C. Hannan, R. M. Paternstro and C. B. Rose, ibid., 80, 5394 (1958).

67) M. C. Markham and K. J. Laidler, J. Phys. Chem., 57, 363 (1953).

68) Y. Fujita, Shyokubai, 3, 235 (1961).

69) R. I. Bickley and K. M. Jayanty, Discuss. Faraday Soc., 58, 194 (1974).

70) S. Okazaki and T Kanto, Nippon Kagaku Kaishi, 8, 404 (1976).

71) R. B. Cundall, R. Rudham and M. S. Salim, Trans. Faraday Soc., 72, 1642 (1976).

72) H. D. Müller and F. Steinbach, Nature, 225, 728 (1970).

73) J. Cunningham, E. Finn and N. Samman, Discuss. Faraday Soc., 58, 160 (1974).

74) F. Feigel, " Spot Tests in Inorganic Analysis", p. 354, Elsevier, Amsterdam (1954).

75) R. I. Bickley and F. S. Stone, J. Catal., 31, 389 (1973).

76) E. Gileadi, E. Kirowa-Eisner and J. Penciner, " Interfacial Electrochemistry", p. 41, Addison-Wesley Publishing, Massachusetts (1975).

77) A. H. Boonstra and C. A. H. A. Mutsaers, J. Phys. Chem., 79, 1694 (1975).

78) J. P. Hoare, " The Electrochemistry of Oxygen", p. 122, Interscience, New York (1968).

79) " Butsuri Josuhyo", p. 227 (Edited by Iida et al.), Asakura Shoten, Tokyo (1969).

80) C. A. Parker, Proc. R. Soc. Lond., 220A, 104 (1953).

81) T. Ohnishi, Y. Nakato and H. Tsubomura, Ber. Bunsenges. Phys. Chem., 79, 523 (1975).